January 2014

A Novel Controlled Release Platform For In Situ Vascular Tissue Engineering

Joseph Thomas Patterson
Yale School of Medicine, joseph.patterson@yale.edu

A novel controlled release platform for in situ vascular tissue engineering

A Thesis Submitted to the
Yale University School of Medicine
in Partial Fulfillment of the Requirements for the
Degree of Doctor of Medicine

by

Joseph Thomas Patterson

2014

Abstract

Autologous tissue engineered vascular grafts (TEVGs) are limited by graft stenosis. Small diameter TEVGs implanted as unseeded scaffolds are prone to failure by occlusive luminal proliferation of smooth muscle cells derived from endothelial precursors within a critical period of two weeks. The development, validation, and application novel platform for controlling TEVG performance by local delivery of peptide and/or small molecule therapeutic agents from the TEVG scaffold is presented with insights into the autologous TEVG biology and development.

We hypothesized that inhibition of TGF-βR1 by local delivery of SB-431542, a competitive inhibitor of ALK5/TGFβR1 signaling, is superior to systemic administration of SB-431542 in the prevention of EndMT-mediated neointimal hyperplastic stenosis of a TEVG during the critical period for graft failure in a mouse model. Specific aims included the development of a multiplexed hybrid drug release platform for delivery of small molecule and/or protein species from a TEVG scaffold; validation of the clinical utility of local versus systemic delivery of SB-431542 in the prevention of TEVG neointimal hyperplastic stenosis in a small animal model; and exploration of TGF-β1 signaling in EndMT and TEVG neointimal hyperplastic stenosis.

Local delivery of SB-431542 or recombinant human TGF-β1 prevented stenosis of a small diameter TEVG. Optimization of the local delivery platform achieved maximum therapeutic efficacy with lower costs than systemic therapy. TGF-β1 signaling is central to endothelial-mesenchymal transition in TEVG dysfunction. Translation of this technology for vascular interventional therapy the hypoplastic left heart syndrome has the potential to improve clinical outcomes.

Acknowledgements

Department of Surgery, Yale University School of Medicine, for guidance, oversight and excellent training; Interdepartmental Program in Vascular Biology and Therapeutics, Yale University School of Medicine, for the facilitates and staff to support this work; and the Yale Core Center for Musculoskeletal Disorders and Bone Histology Laboratory, Department of Orthopaedics and Rehabilitation, Yale University School of Medicine, for histologic processing/embedding supported by National Institutes of Health/National Institute of Arthritis and Musculoskeletal and Skin Diseases Grant AR46032.

I would especially like to thank Christopher K. Breuer, MD, for the inspiration, resources, encouragement, direction, mentorship, and faith that enabled me to undertake these projects; Daniel R. Duncan, MD, MHS, for generously inviting me to complement his stellar work on the subjects discussed herein and kindly treating me as a friend and colleague; Tarek Fahmy, PhD, for warmly welcoming me into his superb research group and guiding the technical development of this project; Tarek Fadel, PhD, and Fiona Sharp, PhD, for generously doing the same while jovially tolerating my incessant consumption of their time, tools, supplies, desk space, chocolate, and patience; and Muriel Cleary, MD, and Mark W. Maxfield, MD, for their contributions to this work, their clinical mentorship, and their continued friendship.

I would also like to thank Michael Simons, MD, for support of these projects; Tai Yi, MD, for his microsurgical skill and warm interest in my professional development; and

Thomas C. Gilliland, B.S., for being an exceptional colleague, frequent partner in crime, great roommate, and true friend.

This work was supported by National Institutes of Health Grants R01-HL 098228, R01-HL 053793, NSF Career Award 0747577, and a National Institutes of Health Autoimmunity Center of Excellence Pilot Award.

Competing interests: Christopher K. Breuer, MD receives research funding from Gunze Ltd., the company that manufactured the full-size scaffolds for the clinical trial. No funding, materials, or other support for the work done in this manuscript was provided by Gunze Ltd.

Foreword

"Age was respected among his people, but achievement was revered. As the elders said, if a child washed his hands he could eat with kings."

— Chinua Achebe, *Things Fall Apart*

As a child, my first dream child was to be an inventor. The light and shoulders of those who made this work possible have carried me toward the realization of that dream. A testament to the clarity of their guidance and the power of our collective efforts is the submission of this work as a component of:

> Yale University, Breuer CK, Fahmy T, Simons M, Chen PY, Duncan DR, Patterson JT. Compositions and method for treating and preventing neointimal stenosis. International Patent Application No. PCT/US2012/40759. 6 December 2012.

My second, somewhat more specific, dream was to be an orthopaedic surgeon-scientist. My intent with this project was always to acquire principles of tissue engineering for application in that field. To continue down the avenue of research detailed herein – which I believe to be a noble endeavor, and a great privilege to have scratched the surface of – would have been to stray from my professional and personal ambitions. As the Breuer research group left Yale for Ohio State University/Nationwide Children's Hospital, I apprehensively submitted an application for a Howard Hughes Medical Institute Medical Research Fellowship to support an additional year engaged in more of this research, work

very remotely related to my intended career path and geographically isolated from the personal relationships that sustain me.

Subsequent clinic experiences in the third year of medical school made it exquisitely clear which professional avenue would be the most fulfilling for me. I chose to decline the HHMI award and complete medical school in four years. This was a choice that I alone made and one that I may always question. I am grateful for the generosity and understanding of those affected by my errant perfidy, and that a more deserving peer at Yale received and made outstanding that fellowship support.

Shamefully absent from this thesis document are the would-be products of that abandoned research year: the likely application of this system toward further investigations of vascular tissue engineering and whatever may have followed.

Joseph Thomas Patterson

31 December 2013

New Haven, CT

Table of Contents

Introduction

Congenital heart disease in the United States

Congenital heart disease is both the most common and most lethal congenital anomaly, affecting 1% of live births in the United States. The leading cause of death among congenital anomalies in the newborn period, congenital heart disease accounts for more pediatric deaths than all childhood cancers combined. Half of all infants born with CHD require surgical intervention to establish cardiovascular continuity that can support growth and prevent development of arrhythmias, developmental disorders, congestive heart failure, and early death[1].

Of the manifold forms of congenital heart disease, the univentricular physiologies including hypoplastic left heart, tricuspid atresia, and pulmonary atresia represent the most severe variety of congenital heart disease. The univentricular physiologies account for the highest treated and untreated mortality as well as the highest treatment costs[2]. Untreated mortality ranges from 70-95% in the first year of life. Surgical correction, in the form of staged palliative operations which moderately reduce mortality at substantial economic, somatic, and neurocognitive costs, remains the gold standard of treatment for these univentricular anomalies[3].

The inadequacy of current care for these diseases warrants the devotion of research resources to further characterization and the development of more effective treatment solutions. Our group has chosen to focus on the most individually burdensome and refractory of the single ventricle physiologies as the disease entity and patient population that stand to reap the greatest gains from such efforts. Hypoplastic left heart syndrome occurs in 0.162/1000 U.S. live births and accounts for only 4-8% of congenital

heart disease[1]. Though one of the least common forms of congenital heart disease, hypoplastic left heart syndrome continues to frustrate clinicians as the most lethal variant of the univentricular physiologies as well as the most expensive type of congenital heart disease to treat[2,4].

Hypoplastic left heart-syndrome

The "hypoplastic left heart" describes a spectrum of left heart hypoplasia with no single pathogenic etiology. The variable constellation of observed anomalies amount to a physiologically inadequate cardiopulmonary system that precipitates universally fatal ischemic congenital heart disease. Variable hypoplasia of the mitral valve, aortic valve, and ascending aorta combined with fibroelastosis of the left ventricle render systemic perfusion dependent upon a single hypofunctional ventricle. Simultaneous arteriovenous mixing via both a patent ductus arteriosus and a nonrestrictive patent foramen ovale are necessary to sustain life. Without treatment, physiologic postnatal ductal closure and falling pulmonary vascular resistance precipitate hypoxemia, acidosis, and shock. Untreated mortality exceeds 95% within the first month of life[5].

The popular mechanistic theory of the development of hypoplastic left heart syndrome describes a primary isolated left-sided defect that disrupts load- or flow-dependent fetal development of other left heart structures. In one example, critical aortic stenosis in the second trimester leads to a normal-sized or dilated left ventricle, retrograde flow across the transverse arch and foramen ovale, and monophasic mitral valve inflow that progresses to left heart hypoplasia and univentricular physiology at birth[6]. Genetic associations with Patau, Edward, Turner, and Jacobsen syndromes, *GJA1*, *NKX2-5*,

NOTCH1, and *HAND1* mutations, and 10 loci of undetermined significance as well as familial associations with bicuspid aortic valve speak to the heterogeneic etiologies of hypoplastic left heart syndrome[7]. Environmental associations are unclear; *in utero* organic solvent exposure has been recently questioned[8].

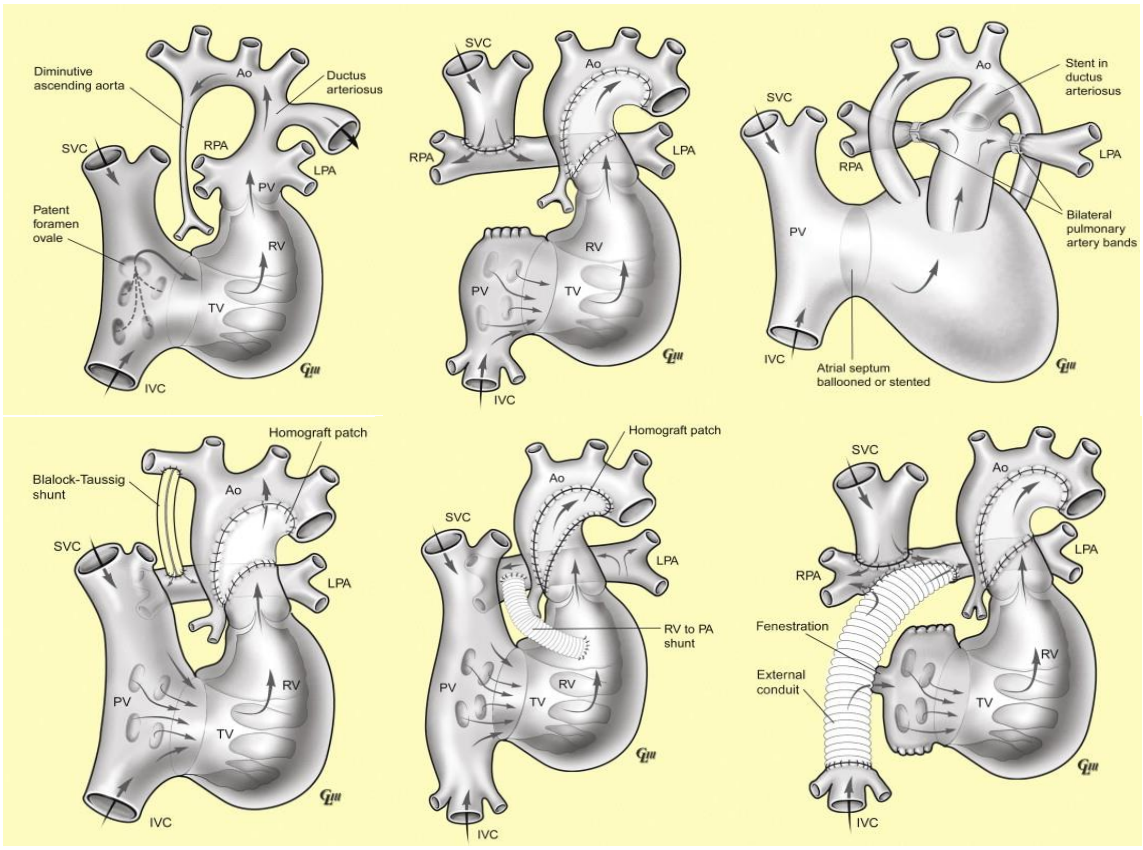

Figure 1. Staged surgical correction of hypoplastic left heart syndrome, (A) Schematic representation of anatomical defects comprising the hypoplastic left heart syndrome. (B) Stage I Norwood procedure. (C) Stage I Hybrid alternative to Norwood procedure. (D,E) Stage II Blalock-Taussig (D) or Sano shunt from right ventricle to right atrium. (F) Stage III modified Fontan procedure with extracardiac shunt from inferior vena cava to right pulmonary artery achieves total cavopolumonary connection. Reproduced with permission from Wolters Kluwer Health (RightsLink license No. 3299370435539)[5].

State of current therapy

Surgical therapy is the mainstay of definitive treatment for hypoplastic left heart syndrome. Five-year survival now approaches 65-77% after staged Norwood palliation[9,10] and 76-84% after cardiac transplant[11,12]. However, mortality on the transplant waiting list varies regionally from 20-40%[13]. The lack of appropriate cardiac donors has solidified the position of staged palliative surgery as the standard of care our arsenal of treatments for this disease[3].

Treatment begins at birth with prostaglandin E_1 to maintain patency of the ductus arteriosus and temporarily preserve systemic circulation. The surgical stage I, the Norwood procedure, is typically performed within the first week of life. The pulmonary artery and pulmonary valve are incorporated into the aortic arch, forcing the right ventricle to assume the functional position of the hypoplastic left ventricle as the physiologic driver of bloodflow to both the systemic and pulmonary circuits. An atrial septostomy routes pulmonary venous return to the right ventricle. A Blalock-Taussig or Sano shunt recirculates mixed venous return and oxygenated blood from the lungs to the pulmonary arteries, enhancing the oxygen saturation of blood entering the systemic circuit at the cost of increased dynamic load for the right ventricle. An alternative hybrid approach to Stage I palliation involves ductal stenting, transcatheter atrial septoplasty, and pulmonary artery banding. Hybrid stage I palliation and improved perioperative management account for recent modest improvements in survival[3].

Stage II palliation is performed at 4-6 months of age. The aortic repair is completed and a bidirectional Glenn shunt or hemi-Fontan shunt is installed to route blood from the superior vena cava(s) directly to the pulmonary artery and unload the right

atrium. The Blalock-Taussig or Sano shunt is taken down to unloads the right ventricle. Stage II boosts arterial oxygen saturation to approximately 80%.

Stage III, the completion, modified, or hemi-Fontan procedure is performed at 2-4 years of age, when the diameter of the pediatric inferior vena is typically 60-80% that of the adult IVC. This operation fully relieves cyanosis by routing the inferior vena cava to the pulmonary arterial circulation with an adult-size (20-22 mm) vascular conduit. The original Fontan, developed in the 1970s, directly connected the right atrium to the pulmonary artery but the size mismatch between the IVC and atrium produced nonlaminar blood flow from the IVC to the atrium and was associated with unacceptably high rates of morbidity and mortality[14,15]. The modified Fontan most commonly performed uses an extracardiac conduit to channel blood from the inferior vena cava directly to the right pulmonary artery. This extracardiac total cavopulmonary connection bypasses the right atrium, thus maintaining laminar flow and increasing the flow of blood through the pulmonary circulation[16]. However, complications arising from the use of synthetic vascular grafts are a leading source of morbidity and mortality[17,18]. No existing vascular graft is an ideal conduit for the extracardiac total cavopulmonary connection. Polytetrafluoroethylene (PTFE or Gore-Tex™) conduits, which have a lower failure rate than Dacron[19], are currently the most widely used vascular grafts for this operation[20]. Autografts are rarely used[21].

Figure 2 (opposite). Gary Kopf, MD, and Toshiharu Shinoka, MD, implant the first tissue engineered-vascular graft for the treatment of pediatric congenital heart disease in the United States. 18 August 2012, New Haven, CT.

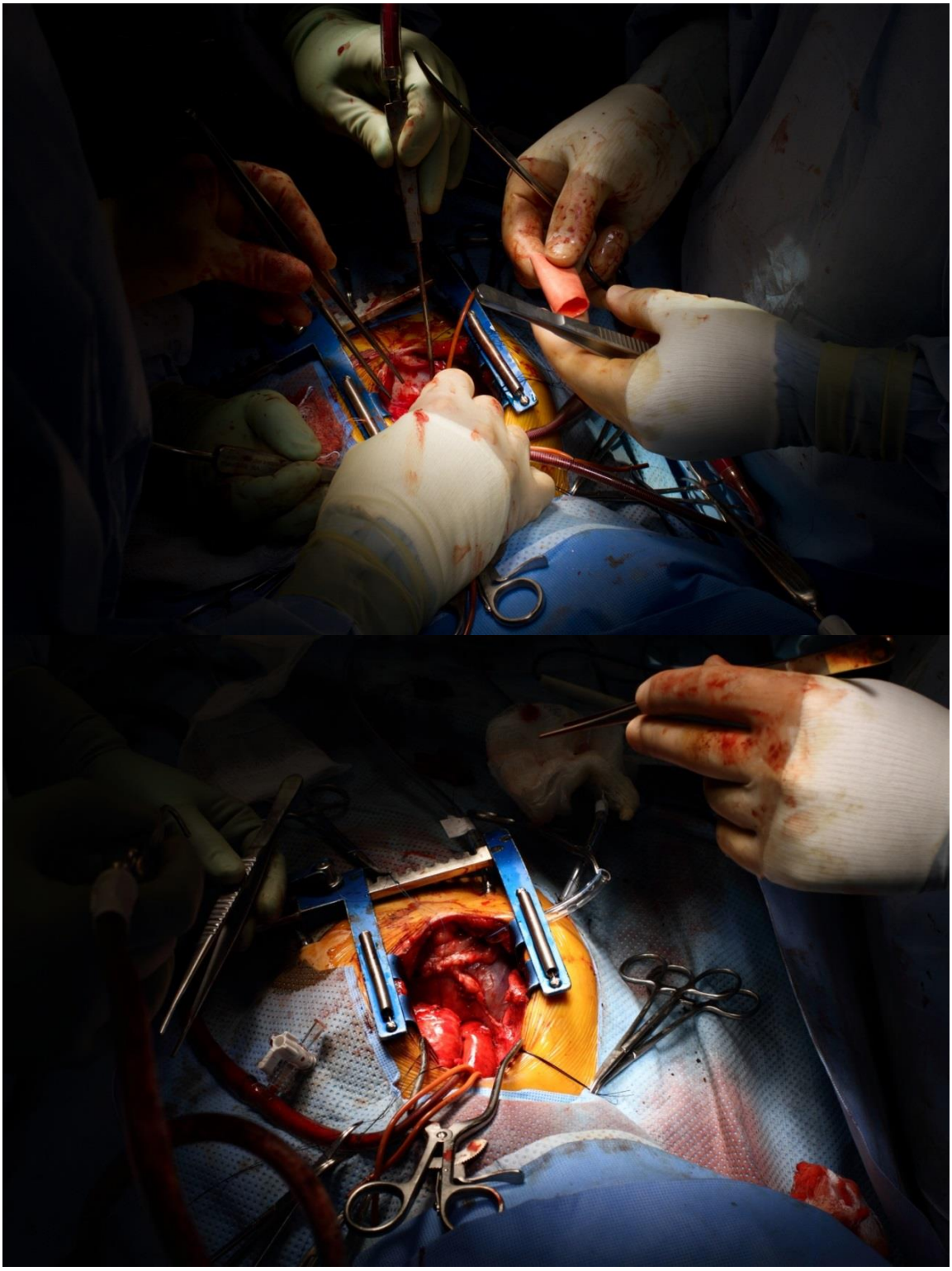

Characterization of TEVGs in animal models

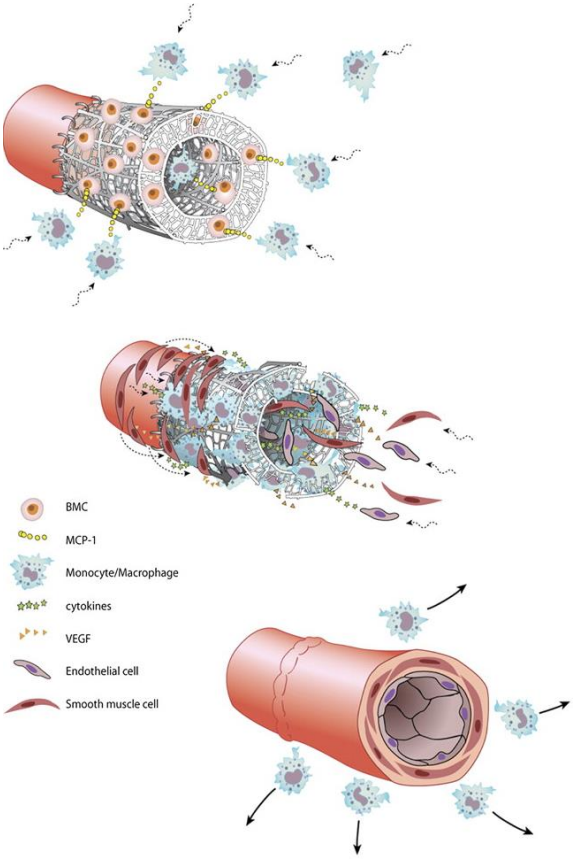

Figure 3. Proposed mechanism of TEVG formation. Reproduced with permission of *PNAS*[22].

Expanded autologous vascular cell lines were seeded onto biodegradable scaffolds of tubularized polyglactin or 50:50 copolymer of L-lactide and ε-caprolactone polywoven (PCLA) mesh sealed with nonwoven polyglycolic acid (PGA) mesh. Seeded or unseeded constructs were implanted as interposition grafts replacing 2 cm sections of the main pulmonary artery in juvenile lambs (polyglactin, N=8) or as thoracic IVC interposition grafts in dogs (PCLA, N=4). At six months after implantation, all seeded scaffolds were patent without anticoagulation, possessed an endothelial lining and overall

morphology resembling native pulmonary artery, and demonstrated non-aneurysmal increase in size. Conversely, unseeded scaffolds formed thrombi and stenosed within two weeks of implantation[23,24]. These results highlighted the importance of cell seeding for TEVG performance but did not elucidate the mechanism by which seeded cells affected TEVG development.

Prior studies by other investigators had demonstrated that vascular grafts seeded with bone marrow cells (BMCs) formed an endothelial monolayer[25]. Rapid endothelization is desirable because healthy ECs reduce the immediate thrombogenicity and immunogenicity of the TEVG and enhance long-term patency[26] . Bone marrow also contains endothelial progenitor cells (EPCs) that may contribute to graft endothelialization and that autocrine signals released by seeded BMCs contribute to vasculogenesis and endothelialization[25,27].

Autologous BMCs enriched for the mononuclear fraction (BM-MNCs) were statically seeded on PCLA/PGA scaffolds, cultured for two hours, and implanted as interposition grafts replacing the intra-thoracic IVC in an adult beagles (N=16). All seeded grafts were patent up to two years without evidence of thrombosis, stenosis or aneurysm formation. Seeded BM-MNCs adhered to the scaffold before implantation. Autologous BM-MNCs could be used as a practical cell source for creating TEVGs, enabling rapid cell harvest without the need for cell culture[28].

Further investigations were performed in a sub-1-mm TEVG mouse model that recapitulates the development of its human and lamb counterparts on a more rapid time scale[29]. When implanted as interposition grafts, these small diameter scaffolds undergo an inflammatory cellularization and remodeling that yields vascular neotissue[22]. Lineage

tracing studies revealed that endothelial and smooth cells migrate in from the adjacent vessel to cover the lumen in concentric layers[30] while circulating macrophages take up residence between the scaffold fibers[31]. Seeding the bare scaffold with BM-MNCs before implantation enhanced graft patency rates and accelerated macrophage and endothelial cell infiltration. However, MRI tracking demonstrated that the seeded cells rapidly departed the scaffold[32]. Seeded cells attracted and influenced the behavior of their cellular successors via a paracrine mechanism involving the deposition of cytokines MCP-1 and PDGF on the scaffold surface[33].

Limitations of cell seeded scaffolds

Manufacturing fully autologous tissue outside of the patient before implantation is expensive; such endeavors require a great deal of time, equipment, facilities, and personnel, and are prone to defects and contamination throughout the fabrication period. Ex-vivo expansion of fully differentiated autologous vascular cell lines can take weeks, and is especially time consuming with tissues derived from patients with vascular disease and other systemic illnesses. Even bone marrow-derived stem cells, which may be harvested, processed, and seeded on a scaffold to create a Fontan conduit that is implanted on the same day as harvesting, requires a large team of personnel and more than eight hours of general anesthesia. Such limitations and challenges make the prospect of an unseeded scaffold very alluring.

Cytokine release from unseeded TEVG scaffolds can modulate the host response to an implanted TEVG to achieve a similar graft phenotype and patency rate as those attained with cell seeded grafts[22]. This observation that cytokine signaling can substitute

for cell seeding in TEVG formation encouraged our pursuit of a "cell-free approach" to tissue engineering whereby scaffolds are modified to slowly release signals that direct host cells to populate the initially acellular scaffold and form a desired architecture[34].

Cell-free paradigm: drug and cytokine release

Integration of a biomedically engineered drug delivery system with the well-studied TEVG scaffold will be central to the fabrication vascular grafts that can control the cellular and molecular processes responsible for neovessel formation. The patient tissues become employees in the assembly line while the scaffold acts as a foreman and blueprint and the cytokines function as instructions.

A cell-free TEVG will eliminate the need for biopsy, *ex-vivo* culture, and seeding of recipient cells – existing challenges to clinical use of TEVG. This will render autologous vessel or bone marrow harvest unnecessary and furnish drastic reductions in economic, personnel, and facility requirements. Moreover, properly stored cytokine-eluting vascular grafts may have shelf lives potentially comparable to PTFE and Dacron grafts. Further characterization of the natural history of TEVG development will inform the selection of cytokines with which to incorporate into scaffolds to improve TEVG performance. The era of an off-the-shelf vascular graft that grows with the patient and behaves like or better than a native vessel is in sight.

The questions, central to this thesis, then become: (a) what process(es) should be targeted to improve TEVG performance; (b) what intervention(s) should be performed; and (c) how can this be implemented without the harvesting of living cells or tissue?

The target: TGF-β1 signaling in endothelial-mesenchymal transition

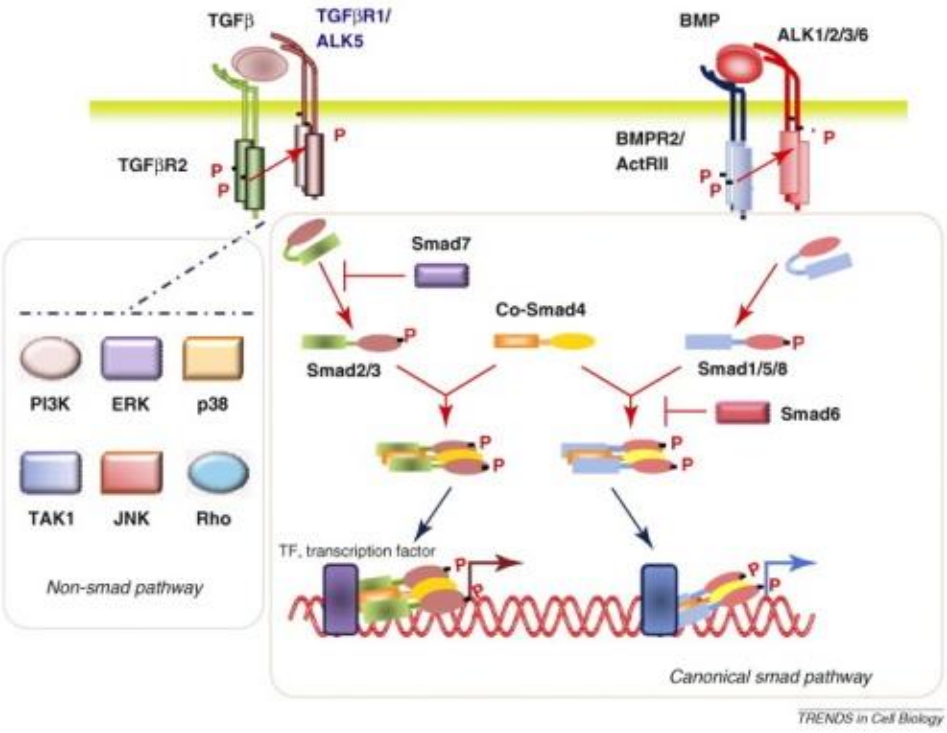

Figure 4. TGF-β signaling pathways in vascular endothelial cells. Reproduced with permission from Elsevier (RightsLink License No. 3299370750146)[35].

TEVGs provide decreasing vascular resistance over time via neovessel growth, but unregulated growth may become pathologic. The primary mode of TEVG failure in humans and animals is luminal stenosis characterized by hyperplastic graft wall thickening and vessel occlusion[36,37]. Excess TGF-β1 protein and mRNA are present in stenosed and unseeded small diameter TEVGs. Our group demonstrated that TGF-β1-driven endothelial-mesenchymal transition (EndMT) is the primary mechanism of TEVG stenosis, which is the sole observed mechanism of TEVG dysfunction[38]. Targeting the EndMT process, then, would be the most logical way to improve TEVG clinical utility.

EndMT is a subset of the epithelial-mesenchymal transition essential during cardiac development and tissue regeneration that also underlies pathologic conditions such as cardiac and hepatic fibrosis and several forms of cancer[39]. EndMT occurs when endothelial cells and endothelial cell progenitors lose their cell junctions, delaminate from the vessel lumen, and invade the underlying tissue. These cells exhibit loss of endothelial markers (CD31, Pecam-1, VE-cadherin) and acquisition of mesenchymal markers (SMA, N-cadherin)[40]. The EndMT process is essential during cardiac development and tissue regeneration but also underlies pathologic conditions such as cardiac and hepatic fibrosis and several forms of cancer[39].

Though its effects are concentration-dependent, TGF-β1 induces mouse endothelial cells to undergo EndMT *in vitro* by signaling primarily through canonical Smad activation and possibly via non-canonical MEK, PI3K, and p38 MAPK pathways[41,42]. Activin receptor-like kinase 5 (ALK5) is the dominant mediator of TGF-β1 signaling in mouse endothelial cells: TGF-β1 → ALK5/ TGF-β1RII → Smad2/3 phosphorylation disrupts endothelial remodeling by suppressing expression of inhibitor of differentiation-1 (Id1)[43,44]. Conversely, TGF-β/BMP → ALK1/TGF-β1RII → p-Smad1/5 enhances vessel remodeling by upregulating Id1 and PAI-1[45]. Pathway dominance of ALK1 vs. ALK5 depends upon TGF-β1 concentration and duration of exposure[44]. Though ALK1 activity *in vitro* elicits responses that are opposite those observed with ALK5 stimulation, the relationship between ALK1 and ALK5 signaling and subsequent endothelial cell behavior is complicated by ligand exposure time and concentration, ALK1/ALK5 codimerization, lateral signaling, coreceptors, and downstream crosstalk[44].

TGF-β1 type II receptors phosphorylate the polarity protein PAR6 which leads to the disassembly of tight junctions[46]. c-Abl and PKC-δ kinases also appear critical for TGF-β-mediated EndMT[47]. However, the effect of TGF-β1 concentration and exposure time on EndMT *in vivo* is unknown. Endothelial and vascular smooth muscle cells constitutively produce TGF-β1, and activation of these cells attenuates endogenous TGF-β1 production.

TGF-β1 promotes mouse endothelial cell proliferation and migration at low concentrations but is inhibitory at high concentrations[35]. This paradox appears related to both the intensity and duration of the signal as well as competition between parallel Smad pathways. Activin receptor-like kinase 5 (ALK5) is the dominant type I TGF-β receptor in endothelial cells; TGF-β11 → ALK5/ TGF-β1RII → Smad2/3 phosphorylation suppresses expression of inhibitor of differentiation-1 (Id1) and obstructs angiogenesis by inhibiting endothelial cell proliferation, migration, and organization. Though some authors described this as an induced "quiescent state," ALK5 → Smad2/3 signaling disrupts endothelial remodeling[43,44].

The intervention: SB-431542, a small-molecule ALK inhibitor

SB-431542 is a potent and specific but poorly soluble inhibitor of Alk5, the dominant type I TGF-β receptor in endothelial cells[48,49]. D. R. Duncan and colleagues demonstrated that systemic administration of this inhibitor in a mouse model of TEVG formation prevents neointimal , mechanistically by inhibiting of endothelial-mesenchymal cell transition[38].

Long-term administration of SB-431542 which has quantifiable activity at range of tyrosine kinases widely distributed through numerous tissues[48] can be reasonably expected to have off-target, potentially deleterious, effects. Moreover, metabolism of this molecule necessitates twice daily intraperitoneal or intravenous dosing, which makes therapeutic use decidedly impractical.

The vehicle: tethered biodegradable microparticles

Controlled release is a powerful method for delivering therapeutic concentrations of biologically active agents directly to the site of their activity by the degradation of or elution from a bulk material, or carrier, placed proximate to that target site[50]. Synthetic biodegradable polymers including the two polymers used in the construction of the TEVG scaffold mentioned previously have been used extensively as controlled release carriers[51]. Micro- and nano-sized synthetic polymer particles are a particularly attractive carrier technology from a design perspective because the fabrication process can be finely controlled to tune the release profile of the therapeutic agent contained within; moreover, such particles can be functionalized with various surface moieties, such avidin, that facilitate particle conjugation with biologically active or functionally useful molecules[52].

However, particles are free floating spheres that may be detached from a surface and thus leave the target site. If particles are to be used form sustained deliver, especially in a high-shear environment such as the lumen of a vascular graft, they would need to be tethered in place.

Coatings of poly-L-lysine conjugated to various targeting molecules have been used to enhance tumor and immunocyte uptake of polymer nanoparticles[53,54]. The

positively charged polyamine group of poly-L-lysine interacts adhesively with the partial negative functional groups of other polymers including as the polyester groups of the poly(glycolic acid) (PGA) and poly((caprolactone-lactic acid) (PCLA) polymer constituents of the TEVG scaffold. The weak hydrostatic and van der Waals forces underlying this adhesion are duplicated over a substantial surface area at the interface of the these polymers, collectively enabling a strong connection between the TEVG scaffold, the linker polymer, and SB-431542-eluting particles.

Statement of purpose

This thesis is an application of biomedical engineering principles and techniques with the above accrued understanding of the pathophysiology of our novel treatment for hypoplastic left heart syndrome for the purpose of developing of the next generation tissue engineered vascular graft. Informed biologic direction of TEVG growth and development *in situ* might enhance graft performance and permit earlier graft use, perhaps even single stage palliative surgery, with further improvements in outcome for this patient population. Understanding of the role of endothelial mesenchymal transition in vascular neotissue formation is expected to yield far wider-ranging applications to the treatment of vascular disease – cardiac and peripheral, pediatric and adult, congenital and acquired.

Hypothesis

Inhibition of TGF-βR1 by local delivery of SB-431542 is superior to systemic administration of SB-431542 in the prevention of EndMT-mediated neointimal hyperplastic stenosis of a TEVG during the critical period for graft failure in a mouse model.

Specific aims

1. Develop multiplexed hybrid drug release platform for delivery of small molecule and/or protein species from previously investigated TEVG scaffold
    a. Encapsulate candidate therapeutics in release vehicle
    b. Tether release vehicle to TEVG scaffold to minimize loss of release vehicle and off target delivery of therapeutic agent
    c. Optimize loading of TEVG scaffold with release vehicle
    d. Characterize release of therapeutics from scaffold
    e. Confirm therapeutics encapsulated in delivery platform retain bioactivity
2. Validate clinical utility of local versus systemic delivery of SB-431542 in the prevention of TEVG neointimal hyperplastic stenosis in a small animal model
    a. Demonstrate local delivery of SB-431542 is more efficacious than systemic delivery of SB-431542
    b. Demonstrate local delivery of SB-431542 is more economical than systemic delivery of SB-431542
    c. Show efficacy of inhibition of TGF-βR1 signaling by SB-431542 is dependent upon the release profile of SB-431542

3. Explore TGF-β1 signaling in EndMT and TEVG neointimal hyperplastic stenosis
    a. Validate previous findings that systemic SB-431542 therapeutically prevents EndMT by replicating results with local delivery
    b. Investigate possible disparate effects of delivery of rhTGF-β1 versus SB-431542 on TEVG formation and clinical function in a small animal model

Methods

All procedures and methods described in this section were developed and performed by the author unless otherwise stated. All figures, photographs, and schematics are original unless otherwise stated.

Scaffold fabrication

TEVG scaffolds were constructed from a nonwoven polyglycolic acid (PGA) mesh (Concordia Fibers) and a co-polymer sealant solution of poly-L-lactide and –ε-caprolactone (P(CL/LA)) as previously described[55]. Briefly, tubular scaffolds were formed by compressing a 6.0 mm x 6.0 mm sheet of nonwoven P(CL/LA) felt between a 21-gauge stainless steel rod (to maintain the inner lumen) and a cylindrical cored-out polypropylene rod. The polymeric scaffolds were coated with a 50:50 copolymer sealant solution of poly–ε-caprolactone-l-lactide (263,800 Da; Absorbable Polymers International, Birmingham, Ala) dissolved at 5% wt/vol in dioxane. Scaffolds were snap frozen at −20°C for 30 minutes lyophilized overnight to remove solvent.

SB-431542-eluting scaffold fabrication

SB-431542-eluting PGA-P(CL/LA) scaffolds were fabricated as above except for the substitution of 5% w/v P(CL/LA) with a 5% w/v P(CL/LA) solution containing 3 mg/ml SB-431542 dissolved in dioxane. The quantity of SB-431542 per scaffold was derived from a density balance calculation such that each scaffold would contain 1/1000 the cumulative mass of intraperitoneal SB-431542 administered as intraperitoneal injections into C57L/B6 over two weeks. Scaffolds were stored at -20°C.

Microparticle synthesis

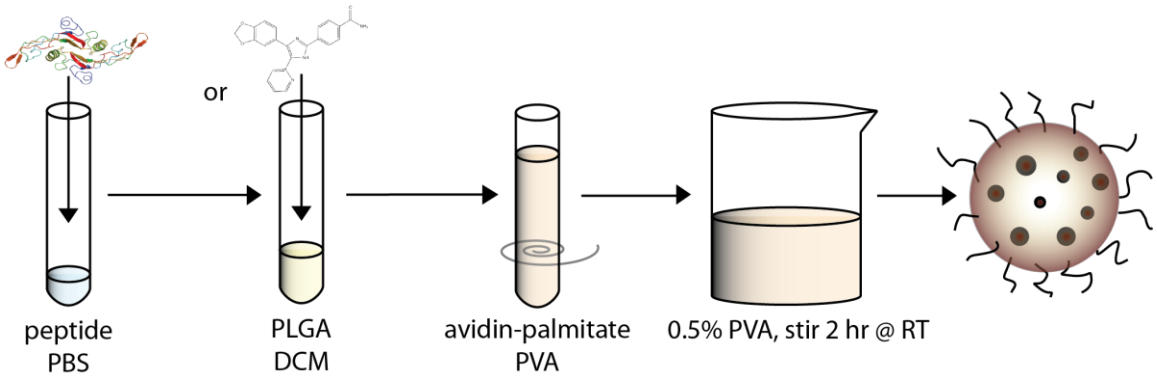

Figure 5. Schematic representation of microparticle synthesis by encapsulation of rhTGF-β1 or SB-431542 in avidin-coated PLGA.

SB-431542 (Sigma-Aldrich Cat. No. S4317) was encapsulated in avidin-coated PLGA microparticles using a modified oil/water single emulsion technique as previously described[52,56]. Briefly, 5 mg of drug and 100 mg PGLA (50/50 monomer ratio, Durect Corp. Cat. No. B0610-2) dissolved in 2 ml chloroform and 200 ul DMSO were added dropwise with vortexing to 4 mL of aqueous surfactant solution containing 2.5 mg/mL polyvinyl alcohol (PVA) (Sigma-Aldrich Cat. No. 363138) and 2.5 mg/mL

avidin−palmitate bioconjugate to create an emulsion containing microsized droplets of polymer/solvent, encapsulated SB-431542 and surfactant. Solvent was removed by magnetic stirring at 20C; hardened microparticles were then washed 3× in DI water and lyophilized for long-term storage at -20C. Null vehicle control avidin-coated PLGA microparticles were synthesized as above without SB-431542.

Recombinant human TGF-β1 (rhTGF-β1) expressed in HEK 293 cells (Humakine, Sigma-Aldrich Cat. No. 8541) was encapsulated in avidin-coated PLGA microparticles using an water/oil/water emulsion technique. 1.0 ug rhTGF-β1 in PBS was encapsulated in 5 mg PLGA microparticles per above. Calculations considering prior studies demonstrating based on 0.2% efficiency of encapsulation of similar hydrophilic protein leukocyte inhibitor factor in this particle system[57] and the relative receptor affinity, dissociation constants, and mass comparisons approximating a five-fold lower order of magnitude difference of physiologically active concentrations of SB- rhTGF-β1 (~1.3 pg/ml).

Microparticle characterization

Microparticle size and morphology were analyzed via scanning electron microscopy (SEM). Samples were sputter-coated with gold under vacuum in an argon atmosphere using a sputter current of 40 mA (Dynavac Mini Coater, Dynavac, USA). SEM analysis was carried out with a Philips XL30 SEM using a LaB electron gun with an accelerating voltage of 10 kV.

Preparation of adhesive peptide tether

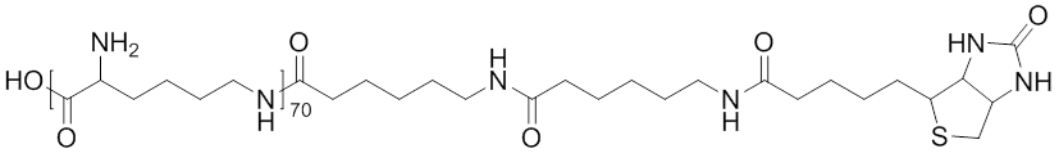

Figure 6. Poly-L-lysine-LC-LC-biotin.

Poly-L-lysine-LC-LC-biotin (pLLB) was synthesized and used as an adhesive peptide tether to enhance loading of PGA-P(CL/LA) scaffolds with avidin-coated microparticles. 1.66 mg EZ-Link sulfo NHS-LC-LC-biotin was reacted with 10 ml of a 0.1 mg/ml solution of poly-L-lysine (MW 70,000-150,000, Sigma-Aldritch Cat. No. P4707) in 1x PBS for 2 hours at 4C, dialyzed in 1x PBS for 72 hours, and stored at 4C.

Loading of TEVG scaffolds with release vehicle

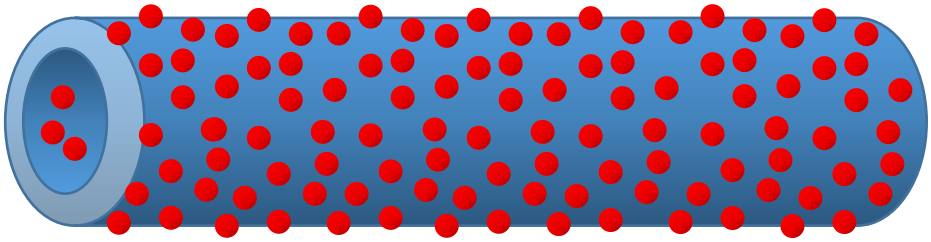

Figure 7. Schematic representation of microparticle decoration of TEVG scaffold.

Nonspecific adsorption of avidin-coated PLGA microparticles to PGA-P(CL/LA) scaffolds not treated with pLLB was titrated by incubating scaffolds trimmed to 5 mm in axial length with 1 ml of 1, 5, or 10 mg/ml of microparticles in 1x PBS for 10, 30 or 60 minutes. Particle-loaded TEVG scaffolds were immediately snap frozen in liquid

nitrogen and lyophilized for 6 hours before imaging. Scaffold loading efficiency was determined with ImageJ software (Image Processing and Analysis in Java, National Institute of Health, Bethesda, MD) from three SEM images per scaffold cross section, inner surface, and outer surface by calculating the mean surface density of particles. The effect of scaffold pretreatment with pLLB on scaffold loading efficiency was assessed from particle loading density as above after PGA-P(CL/LA) scaffolds were incubated with 1 ml of 0.01, 0.1 or 1 mg/ml pLLB for 60 minutes on a rotary shaker, washed 3 times with dH_2O, incubated with 1 ml 5 mg/ml avidin-coated PLGA microparticles on a rotary shaker, washed 3 times with dH_2O, snap frozen in liquid nitrogen, lyophilized for 6 hours, and imaged by SEM. For *in* vitro and *in vivo* studies, PGA-P(CL/LA) scaffolds were incubated with pLLB for 30 minutes at 20C on a rotary shaker, washed 3 times with dH_2O, incubated with 5 mg/ml empty or SB-431542-eluting avidin-coated PLGA microparticles for 30 minutes on a rotary shaker, washed 3 times with dH_2O, snap frozen in liquid nitrogen, and lyophilized for 6 hours before storage in a dessicator.

Characterization of SB-431542 release from microparticles and scaffolds

Total encapsulation was approximated as the amount of SB-431542 released over a 14 day period. Percent encapsulation efficiency was calculated as total encapsulation divided by maximum theoretical encapsulation. 5 mg of avidin-coated PLGA microparticles containing SB-431542, PGA-P(CL/LA) scaffolds trimmed to 5 mm axial length and treated with pLLB and SB-431542-eluting microparticles as above, and SB-431542-eluting PGA-P(CL/LA) scaffolds trimmed to 5 mm axial length were incubated with 400 μl 1x PBS in 2 ml microcentrifuge tubes in triplicate on a rotary shaker at 37C.

Samples were removed at time points of 1, 2, 4, 8, 12, 24, 36, 48, 72, 96, 120, 168, 240, and 336 hours and centrifuged at 13200 RPM for 10 ten minutes. 300 µl of supernatant was drawn and replaced with 300 µl 1x PBS. Concentration of SB-431542 in supernatant diluted with 600 µl 1x PB was determined by spectrophotometry at 320 nm in a quartz cuvette.

Bioactivity of encapsulated SB-431542by p-SMAD immunoblot

SB-431542 was released into 1 ml 1x PBS from 10 mg avidin-coated PLGA microparticles and one untrimmed SB-431542-eluting PGA-P(CL/LA) scaffold in 2 ml microcentrifuge tubes on a rotary shaker at 37C. At 48 hours, samples were centrifuged at 13200 RPM for 10 ten minutes, supernatants were collected and analyzed by spectrophotometry at 320 nm. SB-431542 concentrations were adjusted to 10 µM by dilution with 1x PBS. 3T3 human fibroblasts (Sigma Aldrich, Cat. No. 93061524-1VL) were plated at 500,000/well on a 6-well plate and stimulated at confluence with 700 ul 10 µM SB-431542 in PBS eluted from particles or scaffolds, a stock solution of 10 or 1 µM SB-431542 containing <1% DMSO, 1 or 1x PBS. After 30 minutes at 37C, cells were washed with warm PBS and stimulated with 200 ul 2 ng/ml recombinant human TGF-β1 (BD Biosciences, Cat. No. 354039) for 1 hour at 37C. Cells were lysed with ice cold RIPA lysis buffer containing phosphatase and proteinase inhibitors (PhosSTOP and cOmplete mini, Roche Applied Science, Cat. No. 04906845001 and 04693116001). Cell lysates were collected in 200 µl ice cold 1x PBS by scraping, vortexed for 15 seconds, agitated on a rotary shaker at 4C for 30 minutes, and centrifuged at 12000 RPM for 15 minutes at 4C. Supernatant protein concentrations were determined by DC protein assay

(Bio-Rad Life Science, Hercules, CA) and protein samples were separated by gel electrophoresis with a 12% polyacrylamide gel. Samples were transferred to a PVDF membrane, blocked with 5% milk, and probed with primary rabbit monoclonal antibody against phosphorylated SMAD-2 (ser426/ser428, Cell Signaling Technology, Cat . No. 3010) and secondary goat anti-rabbit IgG (Cell Signaling Technology, Cat. No. 7074). The gel was stripped in stripping buffer (50 ml 62.5 mM Tris-HCl, 2% SDS, 100 mM β-mercaptoethanol) for 40 minutes at 50C with agitation and reprobed with anti-SMAD2/3 as a loading control. The proteins were visualized with ECL exposure on HyBlot x-ray film. Cell culture and blots were performed by Joseph T. Patterson and Muriel Cleary, MD.

Mixed splenocyte scaffold culture

All animal experiments were done in accordance with the institutional guidelines for the use and care of animals as set by the Institutional Animal Care and Use Committee (protocol no. 2007-11160 and 2010-11139]). TEVG scaffolds were trimmed to 5 mm axial length and sterilized under UV light. A 24 well plate was pretreated with 2.5 μg/well anti-CD3 (Sigma Aldrich, Cat. No. SAB4700050). Mixed splenocytes were collected from a 6 week old Foxp3-GFP C57L/B6 mouse (Jackson Laboratory, Bar Harbor, ME), plated at 10^6 cells/well and stimulated with 2.5 ug/well anti-CD28 (Sigma Aldrich, Cat. No. SAB1405583). One PGA-P(CL/LA) TEVG scaffold, one PGA-P(CL/LA) TEVG scaffold treated with pLLB and avidin-coated PGLA microparticles, one PGA-P(CL/LA) TEVG scaffold treated with pLLB and SB-431542 releasing avidin-coated PGLA microparticles, or one PGA-P(CL/LA) TEVG releasing SB-431542 from

the P(CL/LA) phase were incubated with 1 ml stimulated splenocytes for 4 days in quadruplicate. Cell proliferation was assessed by cell titer blue assay. IL-2, IL-10, IL-12, TGF-β, TNF-α, and INF-γ in supernatant were quantified by ELISA. Cells were stained for CD4 on Pacific Blue, CD8 on r-phycoerythrn, and CD25 on on r-phycoerythrn Cy-7. Cell populations were assessed by flow cytometry (LSRII, BD Biosciences).

Pre-implantation scaffold processing

Scaffolds were retrieved from -20°C and lyophilized overnight. Scaffolds were coated with fibrin and thrombin. Scaffolds were sterilized at room temperature under UV light prior to implantation. Scaffolds used for in vitro release studies were not coated with fibrin or thrombin.

Implantation of TEVG scaffolds in C57BL/6 mice

All animal experiments were done in accordance with Yale institutional guidelines for the use and care of animals, and the institutional review board approved all experimental procedures. All animals were housed and cared for in Yale YARC facilities in accordance with institutional policy. Experiments were performed as described in approved IACUC protocol #2010-10835.

TEVG scaffolds were implanted into the infrarenal inferior vena cava (IVC) of 8-10 week old, female mice as previously described [55]. Briefly, female C57BL/6 mice (6-8 wk old, Jackson Laboratory, Bar Harbor, ME) were anesthetized with intraperitoneal injections of ketamine (100 mg/kg) (Hospira, Inc, Lake Forest, Ill) and xylazine (10 mg/kg) (Ben Venue Laboratories, Bedford, Ohio). After preparation and sterilization of

the abdomen with betadine and alcohol, a midline laparotomy incision was made. The IVC was identified and exposed using an 18× dissecting microscope (Zeiss, Thornwood, NY), and the abdominal cavity bathed in heparinized solution (250 U/mL) (Baxter, Deerfield, Ill). Control of the IVC was obtained just inferior to the renal veins and superior to the iliac veins. 10 TEVG scaffolds functionalized with avidin-coated PLGA microparticles, 10 TEVG scaffolds functionalized with SB-431542-eluting avidin-coated PLGA microparticles, and 10 TEVG scaffolds withSB-431542 in the P(CL/LA) phase fabricated as above were implanted as infrarenal IVC interposition grafts via microsurgical techniques. All anastomoses were preformed in an end-to-end technique using 10-0 monofilament nylon sutures (Sharpoint Lab Sutures, Calgary, Alberta, Canada) in interrupted stitches. Adequate hemostasis was achieved before closing the abdominal cavity. Graft recipients were recovered from surgery on warmed pads and evaluated for evidence of hind limb ischemia, paralysis, or acute graft thrombosis before being returned to their cages. All mice were maintained postoperatively without the use of any anticoagulation or antiplatelet therapy. Surgical implantation of all TEVG scaffolds was performed by a single fellowship-trained microsurgeon, Tai Yi, MD.

Explantation and tissue preparation

Mice were sacrificed according to Yale IACUC policy and Infrarenal TEVG IVC grafts were explanted with adjacent tissue by Tai Yi, MD. Explanted grafts were pressure fixed in 10% formalin overnight and embedded in paraffin. Representative grafts (n = 5) from each of the 4 study groups were explanted at 2 weeks and evaluated histologically and by immunohistochemistry. The grafts were pressure perfused before a 24-hour

fixation in 10% formalin as previously described[58]. After fixation, grafts were washed with 1× phosphate-buffered saline and placed in 70% alcohol for an additional 24 hours.

Morphometric analysis

Graft luminal diameters were measured using Image J software. Stenosis was defined as greater than 50% decrease in luminal diameter. Graft occlusion was defined as 100% narrowing of the luminal diameter. TGF-β positive cell area was measured using ImageJ software. Two separate sections of each explant were counterstained with hematoxalin and Gomori trichrome and imaged at 400X magnification.

Histologic analysis

Histologic processing and staining were performed by staff of the Bone Histology Laboratory, Department of Orthopaedics and Rehabilitation, Yale University School of Medicine. Grafts were embedded in paraffin and mounted onto slides (5-μm cuts) allowing for graft analysis. Cellularity and morphometry were evaluated by H&E staining (Sigma). Collagen was identified using Gomori's trichrome stain (Gomori One-Step Trichrome Stain, Dako). Lumen diameter was calculated from Gomori trichrome and H&E-stained sections using Image J software. Further characterization of graft and neovessel cellular composition was conducted using immunohistochemical techniques. Von Willebrand Factor (vWF antibody; Abcam) was used to identify luminal endothelial cells, smooth muscle cells were identified by calponin expression(Calponin antibody; Abcam), and macrophages were detected using F4/80 (BD Biosciences, San Jose, CA). Antibody binding was detected using appropriate biotinylated secondary antibodies,

followed by binding of streptavidin-horseradish peroxidase (HRP) and color development with 3,3-diaminobenzidine (Vector, Peterborough, United Kingdom). Nuclei were counterstained with hematoxylin.

Immunohistochemistry

Primary antibodies included: calponin, clone hCP (Sigma), CD31 (Abcam), smooth muscle α-actin (Dako), vWF (Dako), VE-cadherin (Santa Cruz). Antibody binding was detected using appropriate biotinylated secondary antibodies, followed by binding of streptavidin-HRP and color development with 3,3-diaminobenzidine (Vector). Nuclei were counterstained with hematoxylin.

For immunofluorescence, Two separate sections of each explant underwent triple immunofluorescent staining with DAPI, SMA, and CD31. Goat-anti-rabbit IgG-Alexa Fluor 568 (Invitrogen) or goat-anti-mouse IgG-Alexa Fluor 488 (Invitrogen) was used with subsequent 4',6-diamidino-2-phenylindole nuclear counterstaining. Immunofluorescence was detected using a Leica SP5 confocal microscope.

Cost-effectiveness analysis

Comparison of local and systemic delivery strategies was performed using calculated total multiplicative encapsulation efficiency for each delivery route and current market pricing of $120 per 5 mg SB-431542.

Statistical analysis

Two-tailed paired Student's t-test with the assumption of unequal sample variance was used to compare diameters of the various microparticle species as well as luminal diameters between the different TEVG scaffold groups after explantation. Two-tailed Fisher's exact test was used to compare rates of occlusion between the different TEVG scaffold groups after explantation.

Results

Scaffold characterization

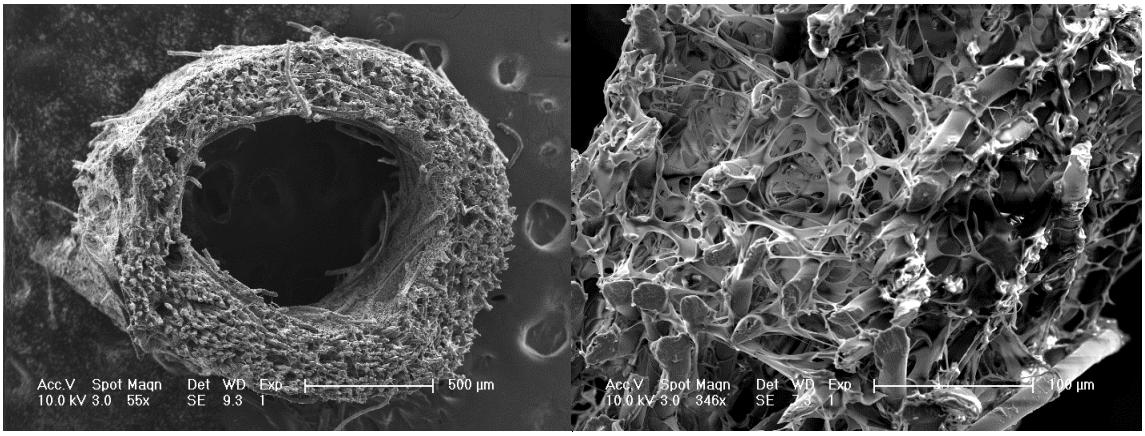

Figure 8. Scanning electron micrograph of tubular PGA-PCLA TEVG scaffold in cross section (A) demonstrating internal and external surfaces available for particle loading and (B) PGA fiber core overlaid with PCLA polymer web.

Microparticle characterization

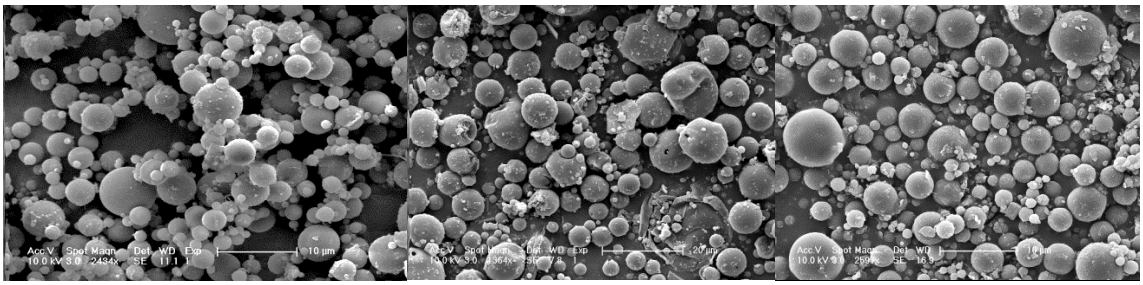

Figure 9. Scanning electron micrographs of lyophilized avidin-coated PLGA microparticles encapsulating (A) null control vehicle, (B) 5 mg SB-431542/100 mg PLGA, and (C) 1 ug rhTGF-β1.

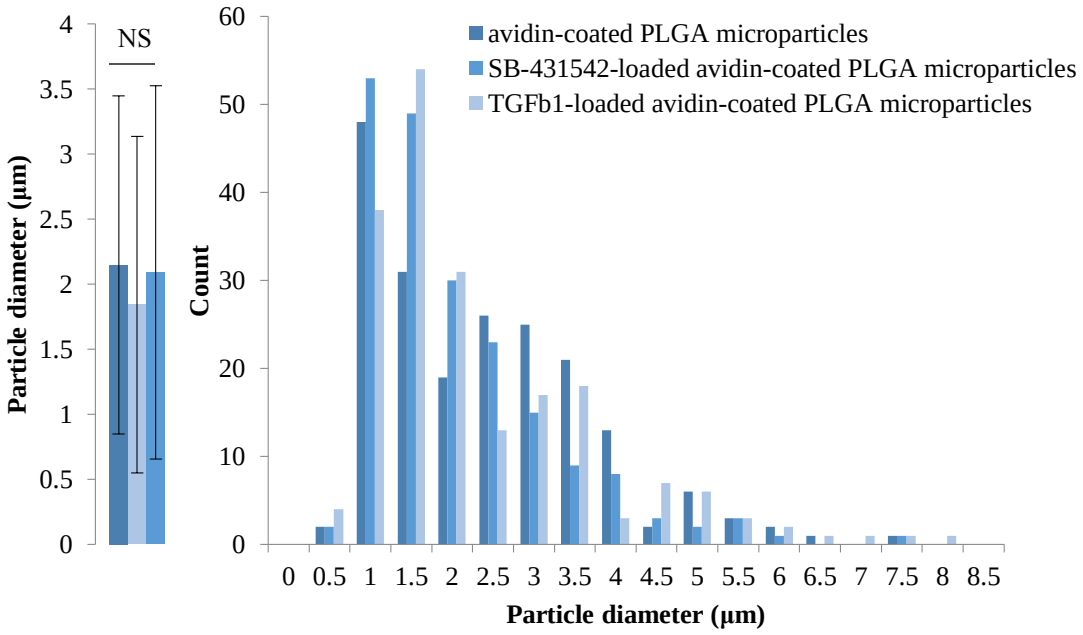

Figure 10. No significant differences in (A) mean diameter (p=0.99) or (B) diameter frequency distribution (p=0.99) of lyophilized avidin-coated PLGA microparticles.

Loading of TEVG scaffolds with release vehicle

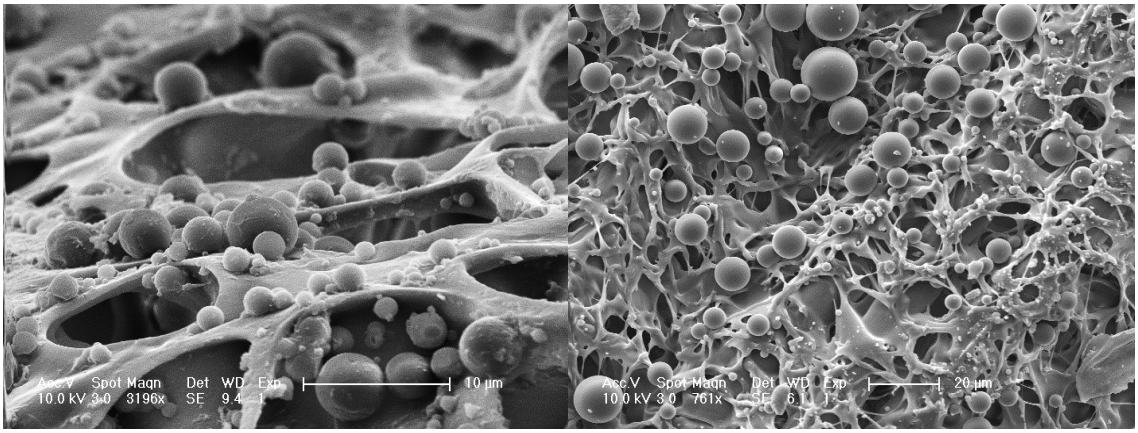

Figure 11. Scanning electron micrograph of tubular PGA-PCLA TEVG scaffold (A) internal and (B) external surfaces after washing demonstrating decoration of TEVG scaffold with poly-L-lysine-biotin and null vehicle microparticles.

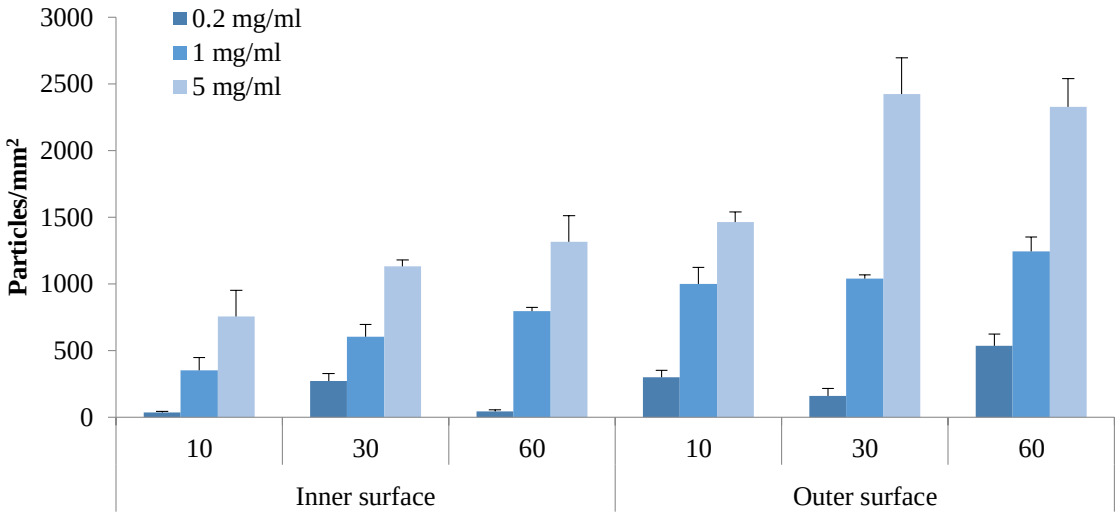

Figure 12. Total loading of TEVG scaffold with null vehicle avidin-coated PLGA microparticles increases with concentration of microparticles in loading solution and scaffold incubaton time in loading solution.

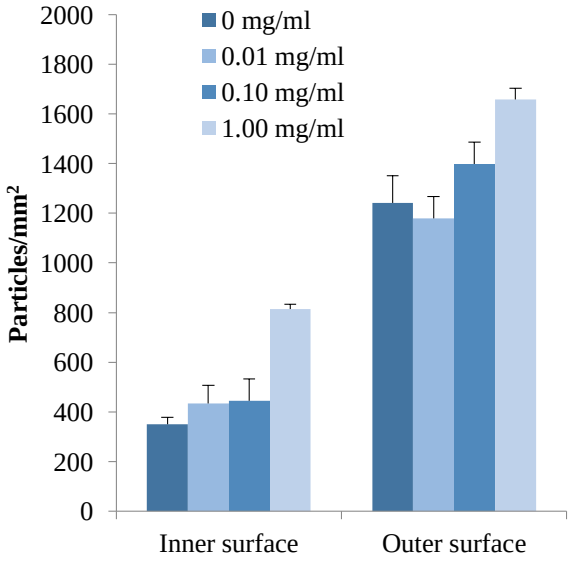

Figure 13. Poly-L-lysine-biotin linker peptide enhances loading density of internal and external TEVG scaffold surfaces with null vehicle avidin-coated PLGA microparticles in a concentration-dependent manner.

SB-431542-elution studies

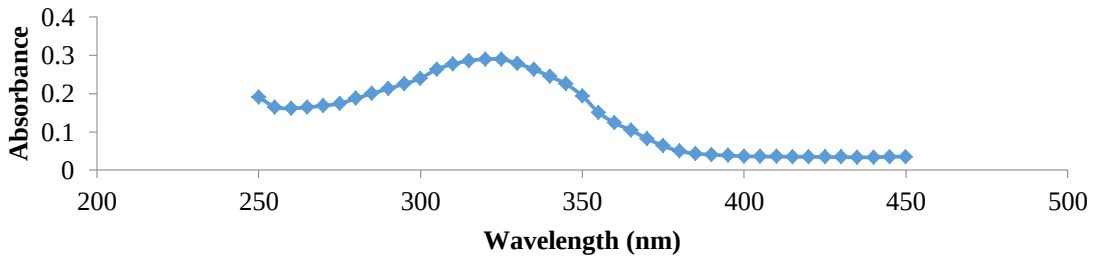

Figure 14. Near-UV spectral photoabsorptivity profile of SB-431542 in PBS demonstrating absorbance maximum at 320 nm.

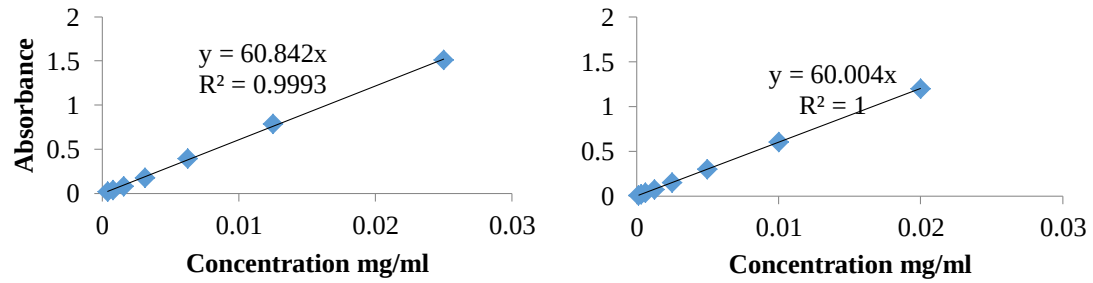

Figure 15. Spectrophotometry standard curves at 320 nm for determining SB-431542 concentration in (A) PBS and (B) DMSO.

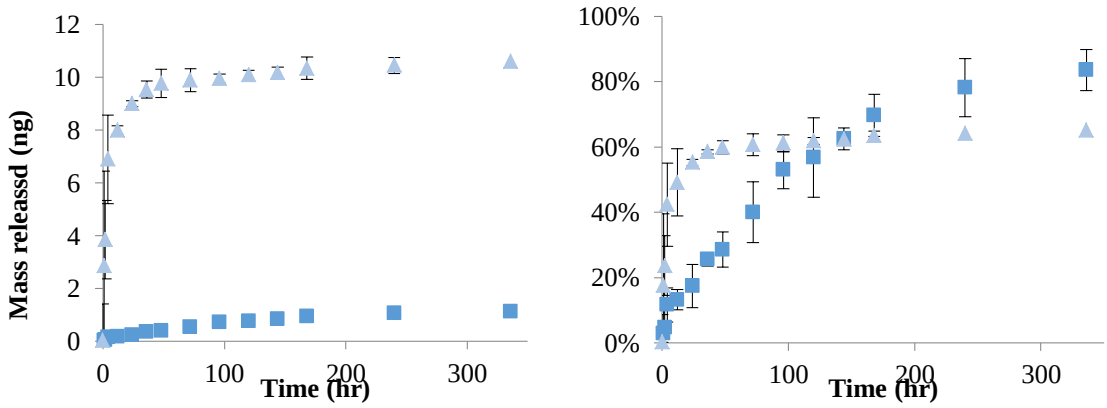

Figure 16. (A) Absolute and (B) fractional release of SB-431542 from eluting scaffolds and from non-eluting scaffolds decorated with eluting PLGA microparticles.

Encapsulated SB-431542 retains bioactivity in TGF-β1 signaling pathway

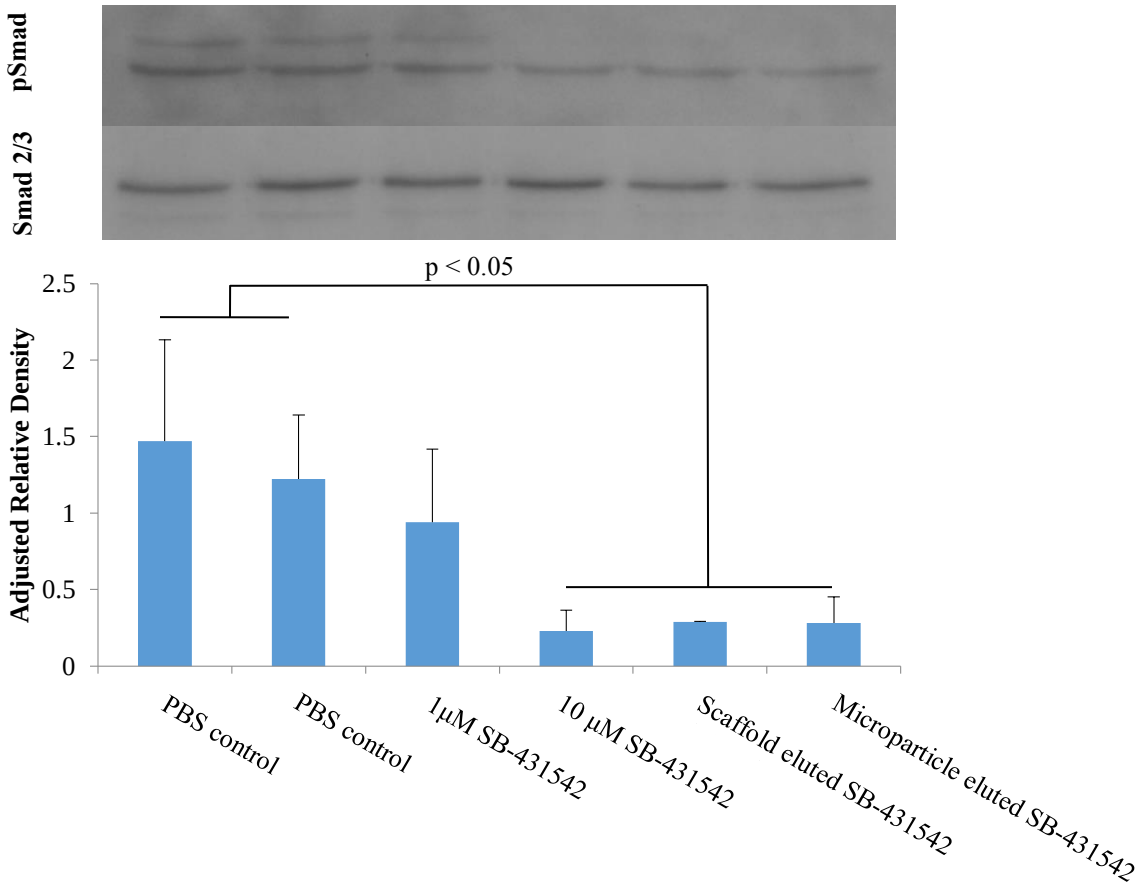

Figure 17. Western blot demonstrating bioactivity of SB-431542 released from scaffolds and microparticles by reduced phosphorylation of Smad3 normalized to Smad2/3. Stock concentrations of SB-431542 and PBS are controls.

SB-431542 delivery systems exert bioactive effects in mixed splenocyte cell culture

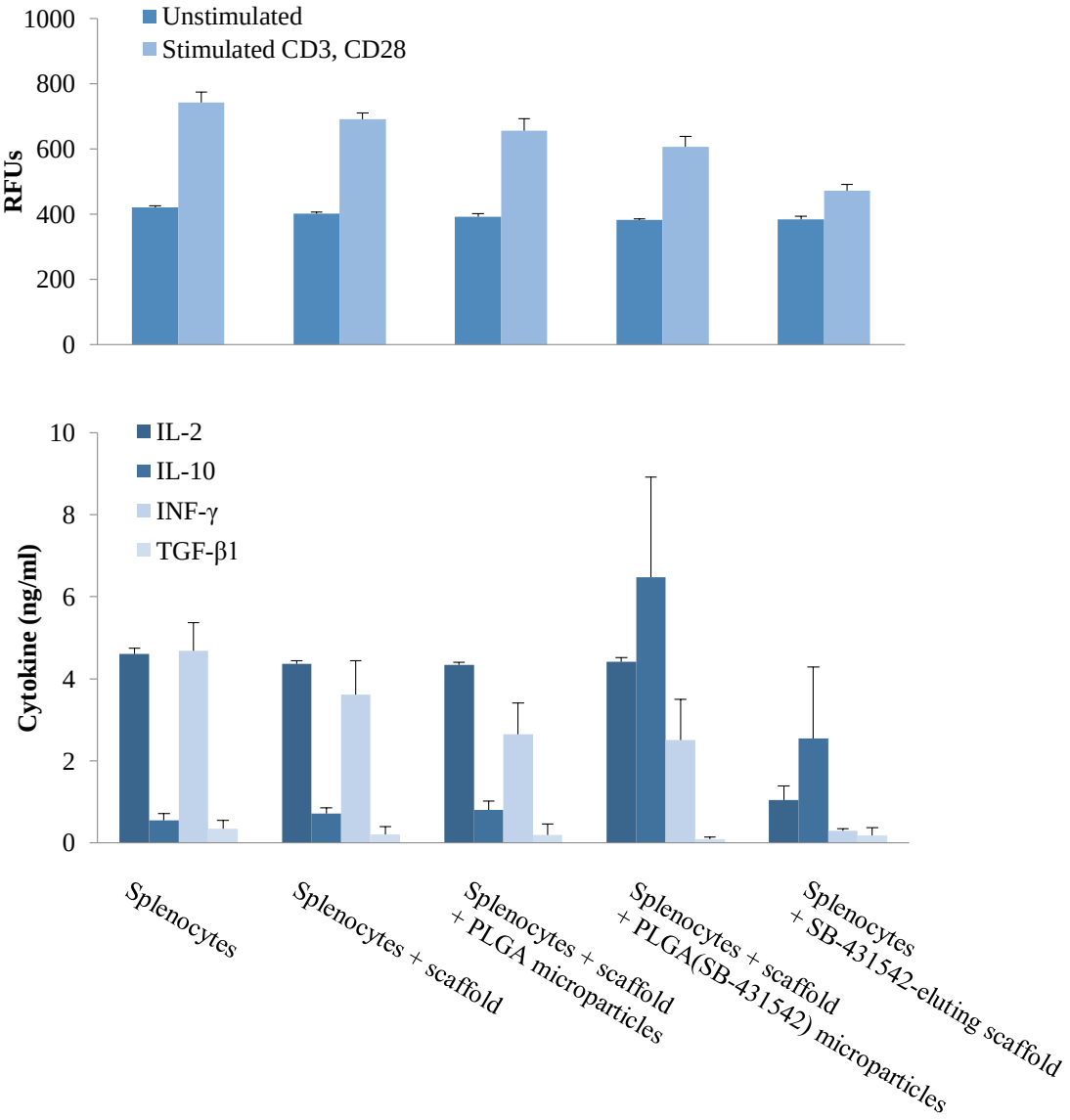

Figure 18. (A) Cell titer blue and (B) ELISA assays demonstrate that SB-431542 eluted from microparticles or scaffolds reduces cell viability and influences expression of cytokines IL-2, IL-10, INF-β, and TGF-β when co-cultured with mixed c57b/l6 mouse splenocytes.

SB-431542 or rhTGF-β1 delivery improves TEVG patency in mouse model

Table 1. Morphometry of TEVGs explanted at 2 weeks

TEVG scaffold	***N***	***Lumen diameter (mm)***		***Patency***
		Patent grafts	***All grafts***	
PGA-PCLA [historical control[22]]	*25*	*0.72 ± 0.09*	*0.37 ± 0.28*	*36%*
PGA-PCLA(SB-431542)	*25*	*0.72 ± 0.06*	*0.52 ± 0.32*	*70%*
PGA-PCLA + systemic SB-431542[38]	*16*	*0.73 ± 0.06*	*0.67 ± 0.16*	*88%*
PGA-PCLA-biotin/avidin-PLGA [control]	*10*	*0.70 ± 0.07*	*0.34 ± 0.31*	*30%*
PGA-PCLA-biotin/avidin-PLGA(SB-431542)	*10*	*0.73 ± 0.08*	*0.73 ± 0.08*	*100%*
PGA-PCLA-biotin/avidin-PLGA(rhTGF-β1)	*10*	*0.76 ± 0.09*	*0.76 ± 0.09*	*100%*

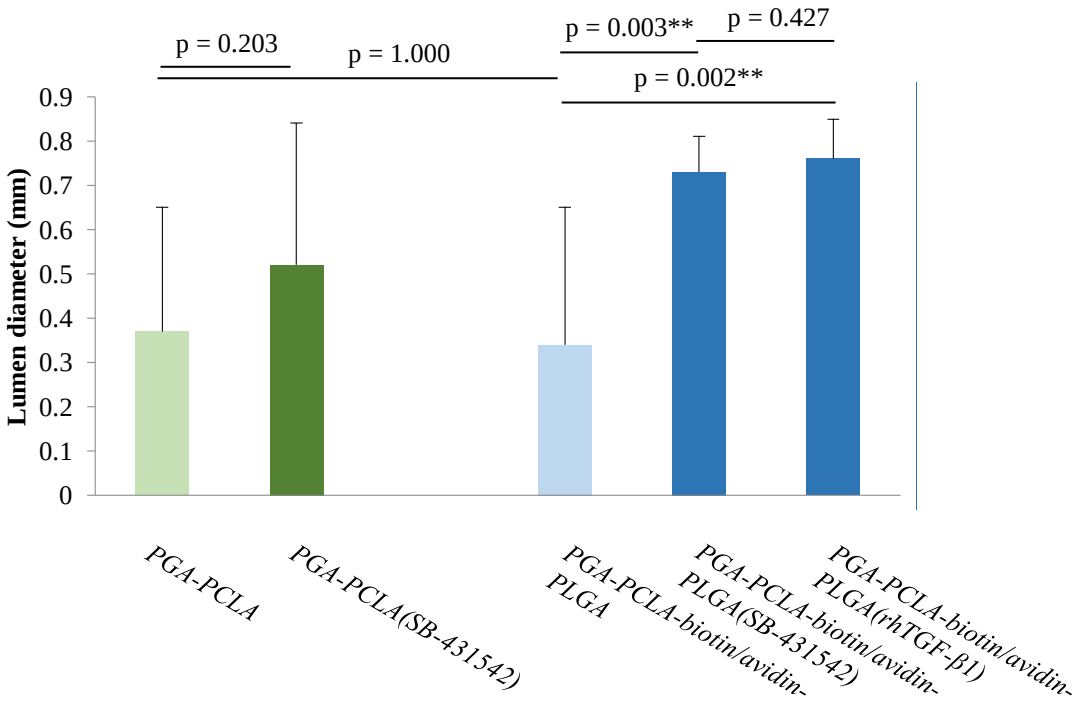

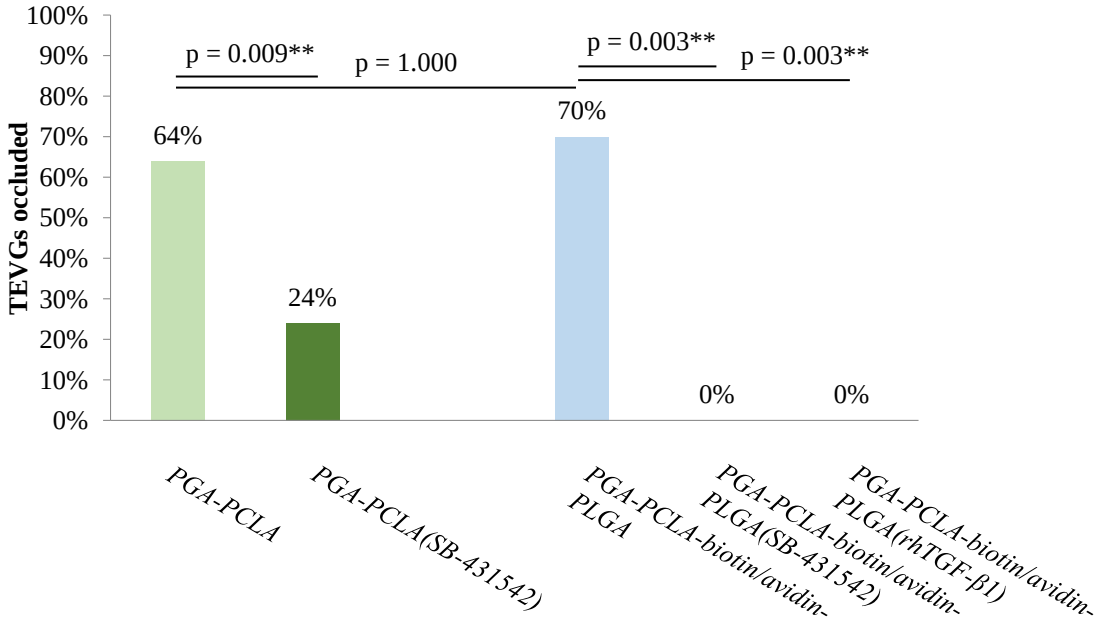

Figure 19. Local delivery of SB-431542 by microparticle or scaffold encapsulation as well as local delivery of rhTGF-β1 by microparticle encapsulation prevent critical stenosis of a tissue engineered vascular graft during the first two weeks after implantation as infrarenal inferior vena cava interposition graft compared with nontherapeutic controls. (A) Luminal diameters are significantly greater with microparticle delivery of SB-431542 or rhTGF-β1 compared to nontherapeuetic controls or scaffolds encapsulation. (B) TEVG occlusion is significantly less common in the first two weeks with local delivery of SB-431542 or rhTGF-β1 by any vehicle, and is not observed with microparticle delivery of SB-431542 or rhTGF-β1.

SB-431542 or rhTGF-β1 delivery inhibits neointimal stenosis and does not disrupt neovessel formation

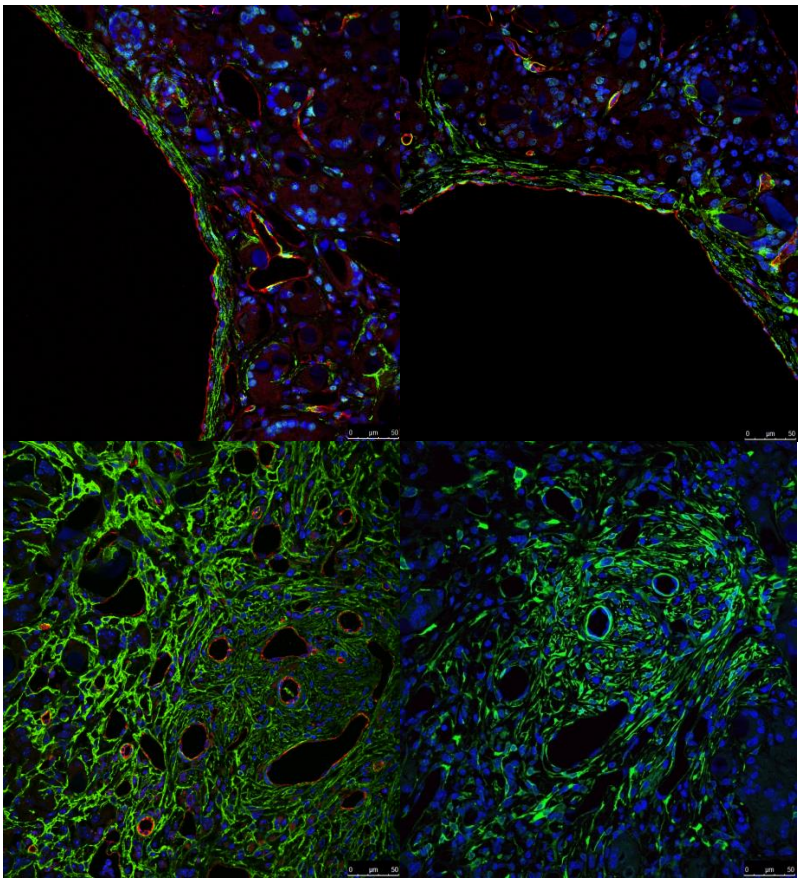

Figure 20. Local delivery of SB-431542 or rhTGF-β1 prevents both mild and critical stenosis of a small diameter TEVG IVC graft by hyperplastic smooth muscle proliferation during the critical first two weeks *in vivo*. Explanted graft sections demonstrated complete concentric layers of endothelium (CD31, red), smooth muscle (SMA, green), and macrophages (F4/80, figure 21). (A) Patent SB-431542 microparticle TEVG, (B) patent SB-431542 dioxane TEVG, (C) critically stenosis SB-431542 dioxane TEVG, (D) critically stenosis control TEVG. Blue is DAPI stain for cell nuclei.

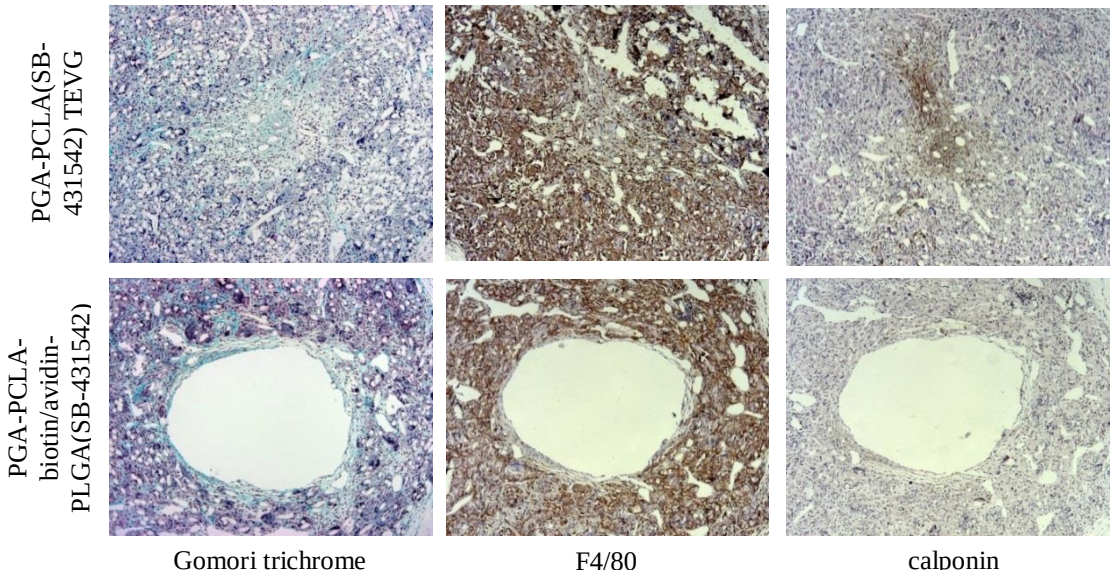

Figure 21. Representative cross sections of explanted occluded SB-431542 eluting TEVG and patent microparticle TEVG demonstrate paucity of macrophage infiltration (F4/80) and high density of collagen (Gomori trichrome) and smooth muscle (calponin) in the hyperplastic luminal obstruction by immunochemical histology. Smooth muscle infiltration and collagen deposition was the sole observed histologic mechanism of TEVG failure. Neither thrombotic nor or embolic occlusion were observed.

Table 2. Comparison of SB-431542 delivery modalities

Delivery route	*Local*		*Systemic*
Delivery vehicle	*PGA-PCLA(SB-431542)*	*PGA-PCLA-biotin/avidin-PLGA(SB-431542)*	*Intraperitoneal injection*[38]
Dosing	*once*	*once*	*10 mg/kg BID IP*
Total administrations	*1*	*1*	*28*
Total SB-431542 consumed per treatment	*100 ug*	*250 ug*	*5.6 mg*
Encapsulation efficiency	21.7%	0.51%	*100%*
Total SB-431542 delivered per treatment	*13.6 ng*	*1.26 ng*	*5.6 mg*
Cost of SB-431542 per treatment	*$2.4*	*$6*	*$134*

Discussion

The results above chronicle the development and validation of a platform for local delivery of therapeutics from a small diameter tissue engineered vascular graft. This thesis is a proof-of-concept that targeted delivery of therapeutics – one small molecule receptor tyrosine kinase inhibitor and one recombinant protein – can be built into a vascular graft and slowly released to control the development and performance of that graft for weeks after surgical implantation. We have also successfully demonstrated that this approach is a viable strategy to enhance the clinical utility of our biologic medical device.

Moreover, the above data document the application of this platform for scientific discovery. I lead the development of this drug delivery system (specific aim 1) to aid Yale School of Medicine alumnus Daniel R. Duncan and our colleagues in the Breuer and Simons labs in validating Dr. Duncan's investigations of the endothelial-mesenchymal transition we observed to underlie stenosis/occlusion of IVC interposition TEVGs in our small and large animal models. Local delivery of SB-431542 from TEVG scaffolds and from microparticles tethered to TEVG scaffolds provided strong supporting evidence that the hyperplastic smooth muscle infiltration of the graft lumens was a TGF-β-mediated process, one that could be intervened upon without the using of seeded cells, and that was not critical for TEVG formation. Application of this system has advanced our understanding of TEVG development *in vivo* and suggested a more complex role for TGF-β signaling in TEVG formation and behavior *in vivo* than previously thought.

We can reject the null hypothesis that local delivery of SB-431542 is noninferior to systemic administration of SB-431542 in the prevention of EndMT-mediated

neointimal hyperplastic stenosis of a TEVG during the critical period for graft failure in a mouse model. However, a demonstration of superior efficacy (specific aim 2a) was not achieved: local delivery of SB-431542 was not significantly more effective than systemic delivery of SB-431542 in the prevention of TEVG neointimal hyperplastic stenosis. There was no significant difference in luminal diameters (0.67 ± 0.16 vs 0.73 ± 0.06 mm, $p = 0.871$) or patency rates (87.5% vs 100%, $p = 0.508$) between systemic intraperitoneal injections of SB-431542 in DMSO vs. microparticle delivery of SB-431542; similar nonsignificant differences were obtained comparing systemic to local elution of SB-431542 from scaffolds. All methods of delivering SB-431542 prevented EndMT and neointimal hyperplastic critical stenosis of the TEVG to some degree (specific aim 3a). Failure occurred exclusively by stenosis with luminal proliferation of SMA+ cells. Disruption of p-Smad signaling by local delivery of SB-431542 prevented this mode of failure, consistent with inhibition of endothelial-mesenchymal transition and smooth muscle proliferation. These experiments were powered to demonstrate feasibility and noninferiority of local versus systemic delivery; the findings obtained support those hypotheses.

A rudimentary cost analysis and review of the methods weakly suggest that local delivery of SB-431542 is more economical than systemic delivery of SB-431542 (specific aim 2B). Local delivery of SB-431542 by drug-eluting scaffolds or scaffold-bound microparticle is roughly an order of magnitude cheaper in material costs and requires considerably less labor, time, and continuing care than serial injections. Microparticle encapsulation is the least efficient (0.51% encapsulation efficiency) in terms of material consumption but also the most effective means of maximizing TEVG

patency in the critical period. Therapeutic administration from the scaffold by either route, which requires no additional preimplantation processing on the day of surgery or additional operative steps and also has less onerous postsurgical care requirements, is inarguable more practical for both care providers and the recipient.

Release studies demonstrated that the eluted SB-431542 was approximately 1/300 the cumulative systemic dose of SB-431542 delivered intraperitoneally, and that 55% of this dose was delivered during the first day. SB-431542 encapsulated in the TEVG scaffolds is likely eluted in two peaks: an early bolus that occurs mostly over the first day post-implantation followed by a gradual release until a second bolus occurs when bulk hydrolysis completes the PGA-PCLA scaffold. Conversely, microparticles tethered to the scaffold delivered a cumulative SB-431542 dose one order of magnitude lower nearly linearly over the first week. The sustained release was significantly more efficacious in achieving the primary outcome of maximum graft patency at two weeks (specific aim 2c). The capability and utility of this system for multiplexed and asymmetric drug delivery from multiple particle species tethered to the scaffold with or without concurrent release from the scaffold polymer remain to be explored.

The investigation of the effect and mechanism of rhTGF-β1 on TEVG formation and function (specific aim 3b) remains incomplete and inconclusive. The core experiment of local rhTGF-β1delivery in the same mouse model was completed and generated the very unexpected and interesting result of also achieving 100% TEVG patency. Unfortunately, the clinical obligations of medical school and the departure of the Breuer lab from Yale University prevented me from completing the necessary experiments to validate those findings. Bioactivity and the release profile of aqueous rhTGF-β1 eluted

from microparticles were never assessed: no data exist to demonstrate that rhTGF-β1 was actually eluted from the encapsulating particles, that any eluted rhTGF-β1 retained physiologic activity, or that rhTGF-β1 was delivered to the target site. Therefore, the unexpected and extremely desirable results obtained with rhTGF-β1-eluting scaffolds should not be accepted.

Nonetheless, the only variable altered in that experiment was the inclusion of rhTGF-β1 in microparticles otherwise identical to those present on the control grafts, decorated on identical scaffolds, constructed by the same operator from the same materials, implanted in the same mouse linage by the same surgeon and same technique. It would seem very possible that rhTGF-β1 was solely responsible for the effect of significantly lower rate of occlusion ($p = 0.003$).

This is an unexpected finding, or possible finding as above. I elected to explore rhTGF-β1 roughly as a control, presuming that if inhibiting the tyrosine kinase of the TGF-βR1/R2 receptors with SB-431542 improved patency then perhaps supplying the agonist would have an opposite, clinically deleterious effect – perhaps increasing smooth muscle hyplerplasia, potentially through EndMT, decreasing patency rates, and degrading clinical utility. Morphologic and immunohistochemical analyses of the explanted rhTGF-β1 TEVGs do not provide suggestions as to why the opposite outcome was observed; histologic architecture is not grossly different from patent TEVGs with or without SB-431542 treatment and cell phenotype densities are not significantly different.

The possibility that rhTGF-β1 may have had a therapeutic effect similar to an antagonist of a mediator of a TGF-β1 signaling pathway suggests that the number ofTGF-β signaling players involved in EndMT and complexity of their relationships may be

greater than we appreciated. Indeed, TGF-β-mediated inhibition of smooth muscle proliferation independent of ALK5/TGFβR1 signaling or ALK signaling altogether. Exploration of these prospects was to be the focus of the "fifth year" research year I ultimately did embark upon.

Future directions

The next step would be to investigate the role of myriad pathways of TGFb signaling in EnMT and neovessel formation. Perhaps selective kinase inhibition of ALK1/2/3/6 → p-Smad1/5 by dorsomorphin[59,60], ALK4/5/7 → p-Smad2/3 by SB-431542[48], or both Smad signaling pathways plus ALK1/ALK5 codimer activity by dorsomorphin and SB-431542 combined administration during TEVG formation would elucidate the relevance of Smad- and non-Smad dependent TGF-β signaling pathways to EndMT and long-term TEVG performance. Small molecule inhibitors would be preferable to protein agonists/antagonists for signaling manipulation in this system as smaller size, resilience to degradation, and lower cost would facilitate screening studies and future local delivery from the TEVG scaffold.

Intervention on the most relevant TGF-β pathway(s) might become the foundation for future strategies to regulate TEVG growth and long-term patency. Endothelial specific reporter mice generated by crossing Tie2-Cre with R26R-LacZ mice would allow colocalization of LacZ+ with mesenchymal markers and quantification of EndMT in harvested TEVG. The effect of systemic administration of each kinase inhibitor or combination on long term patency, stability, and growth could be assessed by quantifying EndMT and diameter of the neovessel lumen and wall layers at various time points.

Local delivery of dorsomorphin and/or SB-431542 from hydrolysable polymer microparticles tethered to the TEVG scaffold[61] would both validate these preliminary studies and provide a cell-free TEVG scaffold amenable to use as an off-the-shelf vascular graft[34]. Scaling up this drug-releasing graft in a lamb model of an extracardiac Fontan shunt comparable in size to that used in a human child would demonstrate that TGF-β1 signaling inhibition improves the function of a TEVG suitable for palliation of hypoplastic left heart syndrome. This would open the door to application for an FDA-sanctioned human clinical trial of a cell-free, off-the-shelf, stable, growing TEVG for patients with hypoplastic left heart syndrome – a major advance over the standard of care.

Given the centrality of TGF-β signaling in embryonic cardiac development, further understanding of TGF-beta signaling in the tissue engineered vascular graft may inform tissue engineering of other cardiovascular structures. Notably, the combined administration SB-431542 and for dorsomorphin as porposed in herein induces the differentiation of endothelial cells into cardiomyocytes[59]. Delivery of these kinase inhibitors from a degradable scaffold may provide the foundation for myocardial patch design. More globally, I envision **drug releasing scaffolds as tissue blueprints** that will underpin the future of the field of tissue engineering. This proposal to explore the complexity of TGF-β signaling in a TEVG through local and systemic delivery of agonists and antagonists will become a model for "cell-free," *in-situ* tissue engineering that combines targeted architectural intervention by surgical scaffold implantation with subsequent tissue building through local-drug-induced cell recruitment and pathway manipulation.

References

1. Lloyd-Jones D, Adams RJ, Brown TM, et al. Heart disease and stroke statistics—2010 update. Circulation 2010;121:e46-e215.

2. Gilboa SM, Salemi JL, Nembhard WN, Fixler DE, Correa A. Mortality Resulting From Congenital Heart Disease Among Children and Adults in the United States, 1999 to 2006Clinical Perspective. Circulation 2010;122:2254-63.

3. Tweddell JS, Hoffman GM, Mussatto KA, et al. Improved survival of patients undergoing palliation of hypoplastic left heart syndrome: lessons learned from 115 consecutive patients. Circulation 2002;106:I-82-I-9.

4. Hospital stays, hospital charges, and in-hospital deaths among infants with selected birth defects--United States, 2003. Morbidity and mortality weekly report 2007;56:25-9.

5. Brawn WJ, Barron DJ, Jones TJJ. Hypoplastic left heart. Paediatrics and Child Health 2011;21:19-24.

6. Mäkikallio K, McElhinney DB, Levine JC, et al. Fetal Aortic Valve Stenosis and the Evolution of Hypoplastic Left Heart Syndrome: Patient Selection for Fetal Intervention. Circulation 2006;113:1401-5.

7. Grossfeld P, Ye M, Harvey R. Hypoplastic Left Heart Syndrome: New Genetic Insights□. Journal of the American College of Cardiology 2009;53:1072-4.

8. Gilboa SM, Desrosiers TA, Lawson C, et al. Association between maternal occupational exposure to organic solvents and congenital heart defects, National Birth Defects Prevention Study, 1997–2002. Occupational and Environmental Medicine 2012;69:628-35.

9. Bove EL. Current Status of Staged Reconstruction for Hypoplastic Left Heart Syndrome. Pediatric Cardiology 1998;19:308-15.

10. Pigula FA, Vida V, del Nido P, Bacha E. Contemporary Results and Current Strategies in the Management of Hypoplastic Left Heart Syndrome. Seminars in Thoracic and Cardiovascular Surgery 2007;19:238-44.

11. Razzouk AJ, Chinnock RE, Gundry SR, et al. Transplantation as a primary treatment for hypoplastic left heart syndrome: Intermediate-term results. Annals of Thoracic Surgery 1996;62:1-8.

12. Chiavarelli M GSRRAJBLL. CArdiac transplantation for infants with hypoplastic left-heart syndrome. JAMA: The Journal of the American Medical Association 1993;270:2944-7.

13. Morrow WR, Naftel D, Chinnock R, et al. Outcome of listing for heart transplantation in infants younger than six months: Predictors of death and interval to transplantation. Journal of Heart and Lung Transplantation 1997;16:1255-66.

14. Fontan F. Atrio-pulmonary conduit operations for tricuspid atresia and single ventricle. Nihon Kyobu Geka Gakkai Zasshi 1978;26:276-84.

15. Fontan F, Baudet E. Surgical repair of tricuspid atresia. Thorax 1971;26:240-8.

16. Marcelletti C, Corno A, Giannico S, Marino B. Inferior vena cava-pulmonary artery extracardiac conduit. A new form of right heart bypass. J Thorac Cardiovasc Surg 1990;100:228-32.

17. Mayer J, Jr, Bridges N, Lock J, Hanley F, Jonas R, Castaneda A. Factors associated with marked reduction in mortality for Fontan operations in patients with single ventricle. J Thorac Cardiovasc Surg 1992;103:444-51.

18. Jonas R. Surgery for congenital heart disease-Commentary//Early results of the extracardiac conduit Fontan operation. Journal of Thoracic and Cardiovascular Surgery 1999;117:695-96.

19. Giannico S, Hammad F, Amodeo A, et al. Clinical Outcome of 193 Extracardiac Fontan Patients: The First 15 Years. Journal of the American College of Cardiology 2006;47:2065-73.

20. Wells W, Malas M, Baker CJ, Quardt SM, Barr ML. Depopulated vena caval homograft: a new venous conduit. J Thorac Cardiovasc Surg 2003;126:498-503.

21. Petrossian E, Reddy VM, McElhinney DB, et al. Early results of the extracardiac conduit Fontan operation. The Journal of Thoracic and Cardiovascular Surgery 1999;117:688-96.

22. Roh JD, Sawh-Martinez R, Brennan MP, et al. Tissue-engineered vascular grafts transform into mature blood vessels via an inflammation-mediated process of vascular remodeling. Proceedings of the National Academy of Sciences 2010;107:4669-74.

23. Shinoka T, Shum-Tim D, Ma PX, et al. Creation Of Viable Pulmonary Artery Autografts Through Tissue Engineering. The Journal of Thoracic and Cardiovascular Surgery 1998;115:536-46.

24. Watanabe M, Shin'oka T, Tohyama S, et al. Tissue-Engineered Vascular Autograft: Inferior Vena Cava Replacement in a Dog Model. Tissue Engineering 2001;7:429-39.

25. Noishiki Y, Tomizawa Y, Yamane Y, Matsumoto A. Autocrine angiogenic vascular prosthesis with bone marrow transplantation. Nature medicine 1996;2:90-3.

26. Kaushal S, Amiel GE, Guleserian KJ, et al. Functional small-diameter neovessels created using endothelial progenitor cells expanded ex vivo. Nature medicine 2001;7:1035-40.

27. Asahara T, Masuda H, Takahashi T, et al. Bone Marrow Origin of Endothelial Progenitor Cells Responsible for Postnatal Vasculogenesis in Physiological and Pathological Neovascularization. Circulation Research 1999;85:221-8.

28. Matsumura G, Miyagawa-Tomita S, Shin'oka T, Ikada Y, Kurosawa H. First Evidence That Bone Marrow Cells Contribute to the Construction of Tissue-Engineered Vascular Autografts In Vivo. Circulation 2003;108:1729-34.

29. Roh JD, Nelson GN, Brennan MP, et al. Small-diameter biodegradable scaffolds for functional vascular tissue engineering in the mouse model. Biomaterials 2008;29:1454-63.

30. Hibino N, Villalona G, Pietris N, et al. Tissue-engineered vascular grafts form neovessels that arise from regeneration of the adjacent blood vessel. The FASEB Journal 2011;25:2731-9.

31. Hibino N, Yi T, Duncan DR, et al. A critical role for macrophages in neovessel formation and the development of stenosis in tissue-engineered vascular grafts. The FASEB Journal 2011;25:4253-63.

32. Harrington JK, Chahboune H, Criscione JM, et al. Determining the fate of seeded cells in venous tissue-engineered vascular grafts using serial MRI. The FASEB Journal 2011.

33. Mirensky TL, Hibino N, Sawh-Martinez RF, et al. Tissue-engineered vascular grafts: does cell seeding matter? Journal of Pediatric Surgery 2010;45:1299-305.

34. Patterson JT, Gilliland T, Maxfield MW, et al. Tissue-engineered vascular grafts for use in the treatment of congenital heart disease: from the bench to the clinic and back again. Regenerative Medicine 2012;7:409-19.

35. Pardali E, Goumans M-J, ten Dijke P. Signaling by members of the TGF-β family in vascular morphogenesis and disease. Trends in Cell Biology 2010;20:556-67.

36. Hibino N, McGillicuddy E, Matsumura G, et al. Late-term results of tissue-engineered vascular grafts in humans. The Journal of thoracic and cardiovascular surgery 2010;139:431-6. e2.

37. Mirensky TL, Nelson GN, Brennan MP, et al. Tissue-engineered arterial grafts: long-term results after implantation in a small animal model. Journal of pediatric surgery 2009;44:1127-33.

38. Duncan DR, Chen P-Y, Patterson JT, et al. Translational Research: From the bench to the bedside and back again. Unpublished data 2012.

39. van Meeteren L, ten Dijke P. Regulation of endothelial cell plasticity by TGF-β. Cell and Tissue Research 2012;347:177-86.

40. Moonen J-RAJ, Krenning G, Brinker MGL, Koerts JA, van Luyn MJA, Harmsen MC. Endothelial progenitor cells give rise to pro-angiogenic smooth muscle-like progeny. Cardiovascular Research 2010;86:506-15.

41. Miyazono K. Transforming growth factor-β signaling in epithelial-mesenchymal transition and progression of cancer. Proceedings of the Japan Academy, Series B 2009;85:314-23.

42. Ghosh AK, Bradham WS, Gleaves LA, et al. Genetic Deficiency of Plasminogen Activator Inhibitor-1 Promotes Cardiac Fibrosis in Aged Mice: Involvement of

Constitutive Transforming Growth Factor-β Signaling and Endothelial-to-Mesenchymal Transition. Circulation 2010;122:1200-9.

43. Goumans M-J, Valdimarsdottir G, Itoh S, et al. Activin Receptor-like Kinase (ALK)1 Is an Antagonistic Mediator of Lateral TGFβ/ALK5 Signaling. Molecular Cell 2003;12:817-28.

44. Goumans M-J, Valdimarsdottir G, Itoh S, Rosendahl A, Sideras P, ten Dijke P. Balancing the activation state of the endothelium via two distinct TGF-[beta] type I receptors. EMBO J 2002;21:1743-53.

45. Seki T, Yun J, Oh SP. Arterial endothelium-specific activin receptor-like kinase 1 expression suggests its role in arterialization and vascular remodeling. Circulation research 2003;93:682-9.

46. Ozdamar B, Bose R, Barrios-Rodiles M, Wang H-R, Zhang Y, Wrana JL. Regulation of the Polarity Protein Par6 by TGFß Receptors Controls Epithelial Cell Plasticity. Science 2005;307:1603-9.

47. Z L, SA J. Protein kinase C delta and the c-Abl kinase are required for transforming growth factor-β induction of endothelial-mesenchymal transition in vitro. Arthritis Rheum 2011;63:2473–83.

48. Inman GJ, Nicolás FJ, Callahan JF, et al. SB-431542 is a potent and specific inhibitor of transforming growth factor-β superfamily type I activin receptor-like kinase (ALK) receptors ALK4, ALK5, and ALK7. Molecular pharmacology 2002;62:65-74.

49. Byfield SDC, Major C, Laping NJ, Roberts AB. SB-505124 is a selective inhibitor of transforming growth factor-β type I receptors ALK4, ALK5, and ALK7. Molecular pharmacology 2004;65:744-52.

50. Baker RW. Controlled release of biologically active agents: John Wiley & Sons; 1987.

51. Uhrich KE, Cannizzaro SM, Langer RS, Shakesheff KM. Polymeric systems for controlled drug release. Chemical Reviews 1999;99:3181-98.

52. Fahmy TM, Samstein RM, Harness CC, Mark Saltzman W. Surface modification of biodegradable polyesters with fatty acid conjugates for improved drug targeting. Biomaterials 2005;26:5727-36.

53. Kim SH, Jeong JH, Chun KW, Park TG. Target-Specific Cellular Uptake of PLGA Nanoparticles Coated with Poly(l-lysine)−Poly(ethylene glycol)−Folate Conjugate. Langmuir 2005;21:8852-7.

54. Thiele L, Rothen-Rutishauser B, Jilek S, Wunderli-Allenspach H, Merkle HP, Walter E. Evaluation of particle uptake in human blood monocyte-derived cells in vitro. Does phagocytosis activity of dendritic cells measure up with macrophages? Journal of Controlled Release 2001;76:59-71.

55. Roh JD, Nelson GN, Brennan MP, et al. Small-diameter biodegradable scaffolds for functional vascular tissue engineering in the mouse model. Biomaterials 2008;29:1454-63.

56. Fahmy TM, Samstein RM, Harness CC, Mark Saltzman W. Surface modification of biodegradable polyesters with fatty acid conjugates for improved drug targeting. Biomaterials 2005;26:5727-36.

57. Gao W, Thompson L, Zhou Q, et al. Treg versus Th17 lymphocyte lineages are cross-regulated by LIF versus IL-6. Cell Cycle 2009;8:1444-50.

58. Roh JD, Sawh-Martinez R, Brennan MP, et al. Tissue-engineered vascular grafts transform into mature blood vessels via an inflammation-mediated process of vascular remodeling. Proc Natl Acad Sci U S A 2010;107:4669-74.

59. Yu PB, Hong CC, Sachidanandan C, et al. Dorsomorphin inhibits BMP signals required for embryogenesis and iron metabolism. Nat Chem Biol 2008;4:33-41.

60. Medici D, Shore EM, Lounev VY, Kaplan FS, Kalluri R, Olsen BR. Conversion of vascular endothelial cells into multipotent stem-like cells. Nature medicine 2010;16:1400-6.

61. Patterson JT, Duncan DR, Cleary M, et al. Local modulation of TGF-β1 signaling prevents critical stenosis in a small-diameter tissue engineered vascular graft. 2012.